SOME PHYSICAL AND STATISTICAL

STUDIES OF METEOR FRAGMENTATION

Richard Eugene McCrosky

(3)

SOME PHYSICAL AND STATISTICAL STUDIES

OF METEOR FRAGMENTATION

A thesis presented

by

Richard Eugene McCrosky

to

The Astronomy Department

in partial fulfillment of the requirements

for the degree of

Doctor of Philosophy

in the subject of

Astronomy

Harvard University

Cambridge, Massachusetts

November, 1955

ACKNOWLEDGEMENTS

DEFINITIONS

Because the terminology in the field of meteor
astronomy has sometimes been confusing it seems advisable
to present the definitions of some words and phrases as they
will be used here.

Both meteor and meteoroid are used to designate the
body producing the meteoric phenomena although, strictly
speaking, a meteor is a phenomenon and a meteoroid is the
body that produces it. This duplication of terms is not a
necessity but it is customary; habit is our only excuse for
using both. Meteoroid is usually reserved for discussions
of the physical or chemical properties of the material
itself. Meteor, on the other hand, often indicates our
concern with the kinematics of the body. Thus, we refer
to the density of the meteoroid and to the velocity of the
meteor.

A photograph of a meteor is called a trail. The trail
appears on the photographic film as a series of dashes
(exposed portion) and breaks (unexposed portion caused by an
occulting shutter). One shutter cycle is the distance, in
space or time, covered by a dash and a break. A meteor
photographed by two cameras at different stations is a
meteor pair. If photographed by one camera only, the trail
is called a single-station meteor.

When observing a bright meteor visually, one often sees a streak of luminosity, after the passage of the meteor, which may persist for a matter of seconds. This delayed luminosity is referred to as the meteor train. Presumably it is caused by recombinations of meteoric and atmospheric ions and atoms. If a train-producing meteor were photographed, the effect of the train would be to fill in the breaks of the trail. The same kind of result would be seen on a meteor photograph if small particles were detached from the meteoroid. These fragmented particles would decelerate with respect to the larger body and, eventually, lag behind. The luminosity derived from the fragments would, in part, fall in the breaks of the trail produced by the meteor itself. We will refer to this phenomenon as the meteor wake. A part of this thesis will be an attempt to show that the above definition serves as a reasonable interpretation of most of the intensity in the breaks. It will be convenient to assume, for the present, that the preceeding explanation is correct. The justification will be presented (Chapter IV) when sufficient data are available.

If the meteoroid breaks into many particles of about the same size, the slight differential deceleration may eventually cause the luminosity to extend over an appreciable length of the trail. In such a case the breaks may be altogether obliterated and we see a phenomenon called "blending." Since this will be observed at the end of the trail, it has been designated as terminal blending.

METEOR NO. 3567

An enlargement (4x) of a meteor trail showing wake and
some terminal blending.

TABLE OF CONTENTS

TABLE OF CONTENTS (continued)

CHAPTER I

BACKGROUND

A. Meteor Problems

The various aspects of meteor astronomy may be
described by a series of questions, not yet answered in
their entirety, that might arise in the mind of any
scientist confronted with the elementary observational
facts. What is the origin of meteors, and their history
in space? What is their physical and chemical structure?
These might be called the astronomical questions. They are
distinct from the physical questions: how do these bodies
interact with the atmosphere, dynamically and physically?
The first two questions are self-explanatory and their
answers, in general, will be descriptive. The last problems
are analytic in nature, and may be enlarged upon immediately.

We require that momentum and energy be conserved in
any process as the meteor penetrates the atmosphere and
collides with the air molecules. The rate of change of
momentum is given by the drag equation:

$$m \frac{dv}{dt} = -\Gamma A (\rho v)\, v, \qquad (1)$$

where

ρ = atmospheric density,

v = meteor velocity with respect to the
atmosphere,

ρv = mass of air penetrated by a unit area of
the meteoroid per second,

A = effective area of the meteoroid, i.e., the
frontal area projected on a plane perpendicular
to the meteor's motion,

Γ = the drag coefficient, a unitless number
representing, in essence, the elasticity of
collisions between the air molecules and the
meteoroid, and

m = mass of the meteoroid.

We may substitute for the effective area the quantity

$$A = Am^{2/3} \delta_m^{-2/3},\qquad (2)$$

where

δ_m = density of the meteoroid, and

A = a shape factor.

Then from (1) and (2) it follows that

$$\frac{dv}{dt} = -\Gamma A \delta^{-2/3} m^{-1/3} \rho v^2.\qquad (3)$$

Given a knowledge of the parameters of this equation, we have
then solved the dynamical problem.

With respect to the energy, we can state _a priori_ that
the energy per second available for all processes is:

$$\frac{dE}{dt} = \frac{1}{2} A \rho v^3.\qquad (4)$$

That the collisions are not elastic is obvious from the
fact that the meteor is observed; that is, some translational
energy is dissipated in the form of radiation. Energy may be

dissipated through dissociation of meteoric and air molecules, excitation, ionization, compression of air, sputtering of atoms or fragmentation of larger particles from the meteoroid surface, and heating of the meteoroid with subsequent vaporization. The rate of mass loss of the meteoroid depends on the last three of these processes: sputtering, fragmentation, and vaporization. The rate at which energy is supplied to each of these processes will be some fraction, Λ_i, of the total rate, or

$$\sum_i \frac{dE_i}{dt} = \sum_i \Lambda_{2i} A \rho v^3,\tag{5}$$

where the subscript i refers to any of the various mass-loss processes. If ξ_i is the energy required to remove a gram of material by a particular process, then the mass loss is given by the equation

$$\sum_i \frac{dm_i}{dt} = -\frac{1}{2}\sum_i \frac{\Lambda_i}{\xi_i} A \rho v^3.\tag{6a}$$

The existing data on sputtering indicates that this method of ablation will be unimportant compared to vaporization. In any case, our observations cannot distinguish between the two processes.

The second physical problem relates to the luminosity of the meteor. From the spectra of meteors we know that much of the light occurs in lines arising from electronic transitions in meteoric atoms. The black body radiation is

small, as it must be for bodies of this size at their
vaporization temperature. These facts alone are sufficient
to suggest that the luminosity is due to collisional
excitation of ablated meteor atoms. The important
theoretical problem, attacked by Öpik (1933), is the
derivation of the luminosity factor, τ. This quantity
relates the available energy to the amount of visible (or
photographic) light produced by the meteor. We assume that
the radiation is proportional to the kinetic energy, with
respect to the colliding air molecules, of the ablated
meteor atoms. Then, the intensity per second is given
by the relation

$$I = -\frac{1}{2}\tau v^2 \frac{dm}{dt}. \qquad (7a)$$

The mass loss, $\frac{dm}{dt}$, in this equation represents only
that mass lost in such a form that a later collision with an
air molecule will produce light. That is, the material must
be lost in atomic (or possibly molecular) form. This type
of loss includes sputtering or vaporization but not
fragmentation or melting with consequent loss of molten
droplets. In these latter cases, the fragments or droplets
must themselves be vaporized before light is produced. The
actual mass loss which is measured at any time is, on the
basis of Öpik's theory, an atomic particle loss. We will,
then, rewrite equation (6a) in the form,

$$\dot{m} = \frac{dm}{dt} = -\frac{\Lambda}{2\zeta} A\rho v^3 = -\frac{\Lambda}{2\zeta} A\delta_m^{-2/3} m^{2/3}\rho v^3, \qquad (6b)$$

where the mass loss and the constants Λ and ζ now represent the sum of those processes which ablate material from the meteoroid in the form of atoms or molecules. Substituting this in equation (7a), we derive the luminosity equation:

$$I = \frac{\tau}{4}\frac{\Lambda A\delta_m^{-2/3}}{\zeta} m^{2/3}\rho v^5. \qquad (7b)$$

Öpik's semi-classical approach could, in theory, be improved upon by quantum mechanical methods. Few experimental data exist on collisional excitations by neutral atoms of this energy range ($\sim$100 e.v.). Consequently, Öpik's results are still in use, although we must consider this value as only a first approximation to the truth. He found the luminosity factor to vary as:

$$\tau = \tau_o \, v \qquad (8)$$

where τ_o = constant. Therefore

$$I = -\frac{\tau_o}{2} v^3 \frac{dm}{dt} = \frac{\tau_o \Lambda A\delta_m^{-2/3}}{4\zeta} m^{2/3}\rho v^6. \qquad (9)$$

Thus, the physical problems become one of finding values for Γ, A, Λ, δ_m, ζ, and τ_o. The atmospheric density, ρ, has been obtained from recent rocket measurements (The Rocket Panel, 1952) and will not be considered as an unknown here.

B. <u>The Meteor Data</u>

To answer our questions we may call on theoretical, observational, and experimental techniques. We will review these tools briefly. We have already spoken of theoretical approaches to the problems of luminosity.

Observational data may be obtained photographically, visually, or by means of radar reflections from the ion column formed by the meteor. The last two sources will not concern us here. Let it suffice to state that the radar method can give us (1) the range of the meteor at the point of closest approach to the receiver, (2) the apparent angular velocity of the meteor at this point, (3) the line density of the ion column at this point and, under certain conditions, (4) the radiant or radiant distance of the measured point and from this, the space velocity of the meteor.

The value of visual observations was greatly reduced by the advent of the far more accurate photographic techniques. Furthermore, some statistical problems whose solution required the large number of visual observations are now best treated with the still more numerous and more accurate radar observations. And it is certainly not amiss to assume that statistical problems concerning the optical properties of meteors can be most accurately approached through reductions of large numbers of faint photographic meteors by the methods used in this work.

In the photographic program at Harvard, a pair of fast, wide angle cameras, 18 miles apart, are used to photograph the same meteor. The distance between the cameras is the baseline that supplies the distance scale. To provide a time scale, a shutter occults the optical system at known intervals, and intersperses the meteor trail with a series of breaks. Measures of these photographs yield directly the radiant and the height, velocity, and intensity as a function of time. In Chapter II we will describe an approximate method for finding these quantities. A summary of the more accurate method utilized by Whipple and Jacchia (in press) may be found elsewhere.

Photography of meteor spectra and time-lapse photographs of meteor trains have given additional information on the meteoric process. The reader interested in details may consult papers by Millman (1952, 1953) and by Cook and Millman (1955) for spectroscopic data, and papers by Whipple (1953) and by Liller and Whipple (1954) for the meteor train data.

Wind tunnel studies and measures of the flight and luminosity of high-speed pellets (Thomas and Whipple, 1951) (Rinehart, Allen and White, 1952) have yielded experimental results. Such work has given a good estimate of the drag coefficient, Γ, and set some limits on the coefficient of heat transfer, Λ.

We might also expect to include in the experimental data the results of studies of meteorites which yield values for the meteoric density, δ_m, the heat of vaporization, ζ, and, of course, chemical and physical composition in general. In that these data represent the only case where an astronomical result could be obtained directly in a terrestrial laboratory, they are unique. Unfortunately, however, they are misleading, for, as Whipple (1952) has shown for meteoric densities and as will be shown here for their physical structure, meteorites are not representative of meteors in general. Indeed, the difference between photographic meteors and meteorites could hardly be greater. It is difficult to find any other natural substance on the surface of the earth with the tenacity of an iron meteorite and, if our results are correct, material as fragile as the ordinary cometary meteoroid could not long exist under conditions on the earth's surface.

C. Some Important Earlier Work

Let us assume that the fundamental qualities that describe a meteor - the radiant and the velocity, height, and intensity as a function of time - have been measured, and let us apply the theory outlined in the first section to determine what we can about the meteor problems.

The mass of the meteoroid at any time is given by the integration of equation (9):

$$m(t) = \frac{2}{\tau_0} \int_t^\infty \frac{I}{v^3} \, dt, \qquad (10)$$

where $t = 0$ when the meteor is first detected. A lower
limit of $t \longrightarrow -\infty$ is used to express the mass, before any
ablation has taken place. Since the intensity of the meteor
at the limit of detectability is usually very small compared
to its maximum intensity, even a bad extrapolation of the
light curve into the unobservable region will produce only
a small error in the initial mass, $m(-\infty)$. (For convenience,
this quantity is written as m_∞. A similar notation, V_∞, is
used for the velocity of the meteor before it has suffered
any deceleration.)

With the mass known, we may use equation (3) to determine
the air density, ρ, to within the error imposed by our
ignorance of the constants of that equation. Such data were
among the first to give us information of the upper
atmosphere (Whipple, 1939). Today, we can assume the density
to be known from rocket measures and can invert the equation
to obtain information about the meteor in terms of an
observed constant, K_1:

$$K_1 = \Gamma A \delta_m^{-2/3} = -\rho^{-1} v^{-2} \left(\frac{2}{\tau_0} \int_t^\infty \frac{I}{v^3} dt \right)^{1/3} \left(\frac{dv}{dt} \right). \quad (11)$$

Or, if we consider τ_0 to be an unknown as well, we get

$$K_1 \, \tau_o^{1/3} = - \rho^{-1} v^{-2} \left(2 \int_t^{\infty} \frac{I}{v^5} dt \right)^{1/2} \left(\frac{dv}{dt} \right). \qquad (12)$$

Whipple (1955) found that the observed values of this overall constant could not be satisfied by use of values of the individual constants thought to be reasonable. Specifically, if we accept the value of ΓA measured by Rinehart, Allen and White (1952) for high speed pellets, and the value of the luminous efficiency determined by Öpik, then the corresponding value of the meteoric density is about $0.3 \ gm/cm^3$. If the luminous efficiency is increased to the maximum possible value (an efficiency of unity for the fastest meteors), the density is $1.7 \ gm/cm^3$ - a value considerably less than that found for any meteorite. Such a value tempts us to speculate on the structure of a cometary meteoroid, but we will limit our discussion at this time to two remarks. First, Whipple has pointed out that these values are in qualitative agreement with his icy-conglomerate Comet Model (1950). Second, our knowledge of materials formed at near zero temperatures and pressures is admittedly small. One should guard against any preconceived ideas, based on his familiarity with terrestrial substances, when discussing the result cited above.

Another observationally determined constant, relating to the rate of mass loss, may be found. Dividing equation (6)

by equation (3), we obtain the relation

$$\frac{\wedge}{2\Gamma\xi} = \sigma = \frac{\dot{m}}{mv\dot{v}} = \frac{I}{\int_{-\infty}^{+\infty}\frac{I}{v^5}dt \; v^4 \dot{v}} \; . \tag{13}$$

This may be integrated to give:

$$m = m_0 \; e^{-\frac{\sigma}{2}(v_0^2 - v^2)} \; . \tag{14}$$

(14)

The measured values of σ, as determined by Jacchia, range from about 10^{-12} to greater than $10^{-10.5}$ ($\frac{sec^2}{cm^2}$). If we assume Rinehart's value of $\Gamma = 0.42$ and use the vaporization energy of stone or iron, say $5.6 \cdot 10^{10}$ ergs/gram, the observed values of σ determine a value of $\wedge$ (see Table 1).

Table 1

The Heat Transfer Coefficient $\wedge$ as

Determined from Observed Values of σ.

$\sigma (sec/cm)^2$	$\wedge$
10^{-12}	.047
$10^{-10.5}$	1.49

Not only is the range in values large, but the largest derived value exceeds the theoretical limit of unity for the fraction of their energy that the incoming air particles may transfer to the meteor. Furthermore, if we transfer all

energy, we transfer all momentum and our assumed value of Γ must be unity as well. This more than doubles the value of Λ in the extreme case and intensifies the discrepancy.

It might be suggested that the answer to the problem lies in the mode of ablation and indeed it probably does. Models of ablation, other than direct vaporization from the meteoroid, have been considered in order to explain the range and discrepancy in the observed values of σ. R. N. Thomas (1952) first showed that, on the basis of the classical heat transfer equation as applied to iron meteors, the heat conductivity toward the center would proceed too rapidly to allow the surface temperature to reach a value great enough to produce any appreciable amount of vaporization. He then considered the possibility that vaporization or melting and the shedding of droplets from a reaction zone at the surface was responsible for the loss of energy from the surface rather than the conduction of heat inward. He concluded that <u>if</u> droplets were dispersed from the surface, they would be small and the energy needed for this type of ablation would approach that required for vaporization. Thomas felt that only fragmentation, which can be nearly an energy-free process, could account for the scatter of the σ - values.

Although it is true that the meteoroid can lose material at the expenditure of less energy by melting or fragmentation, nevertheless the observations require that the material be in

the form of atomic particles at the time the luminosity is produced; i.e., if droplets do form, additional energy must still be supplied to vaporize the liquid, for we can observe only that mass which eventually reaches the vapor phase. The effect of the increased surface area due to the droplets or fragments will, however, affect the vaporization rate.

Following Jacchia's (1949) demonstration that meteor flares involved a loss of mass from the meteoroid, Henry J. Smith (1954) analyzed several bright meteors that displayed bright flares. He concluded that meteor flares were caused by the sudden fragmentation of a large number of small particles, of the order of 10^{-6} grams each.

Jacchia (1955) then made the significant contribution of the concept of the continuous fragmentation of meteors. His approach to the problems was primarily the empirical one needed to find some correction to the atmospheric densities derived from meteor decelerations.

Jacchia's early results, with bright meteors, agreed statistically with the values of atmospheric density obtained from rocket flights. For any one meteor which gave decelerations at more than one point, the density gradient found from the meteor data also agreed with the rocket data gradient. However, later results obtained from faint meteors photographed with the Super-Schmidt cameras showed distinctly anomalous decelerations. Although the decelerations near the beginning points of these meteors often gave a reasonable

value of the density, the meteors displayed too rapid a
rate of deceleration, yielding density gradients that
could not be reconciled with either the previous meteor
or rocket results. We cannot improve upon Jacchia's
own description of the solution of this discrepancy:

> "Fragments can be detached from the surface
> of larger meteor bodies without destroying their
> unity; but if fragments of similar size are
> detached from small bodies, this may mean their
> complete disruption into cluster of fragments.
> Larger meteors, then, will disintegrate only
> toward the end of their trajectories, while among
> fainter meteors the breakup may occur at earlier
> stages, even at the very beginning of the visible
> trail. What we obtain by integrating the bright-
> ness of a faint meteor is not the mass of a single
> body but a function of the total mass of all the
> fragments. The observed meteor deceleration, on
> the other hand, is the average deceleration of the
> brighter fragments and therefore larger than the
> deceleration of a single, unfragmented body."

In this brief review of some recent work, we have
touched on two aspects of the meteor problem which we intend
to amplify in this thesis. Whipple's discussion of the
densities makes the assumption of fragile meteors reasonable,
while the conclusions of Thomas and Jacchia on fragmentation
almost necessitates the assumption. Our aim will be, in
effect, to strengthen the concept of the fragile cometary
meteoroid and to initiate a quantitative study of meteor
fragmentation.

D. A Semi-Qualitative Approach to the Relationship Between Fragmentation and the Parameter σ.

Let us consider two special cases of meteoroids with a large surface-to-mass ratio. First, suppose the "meteoroid" to consist of a large number of small particles of the same size; each one interacts independently with the atmosphere but in the entire swarm the particles are sufficiently close together to allow our cameras to record them as a moving point source of light. We may think of this swarm as originating from a single body that has either fractured or melted and broken into droplets in the fashion of an over-sized rain drop. The mechanism is unimportant; the end result is an unlikely array which we wish to use to describe one extreme of subdivision. The question we wish to answer is: What value of σ would such a meteor yield? The observed deceleration would be that for an individual particle, since each particle reacts independently with the atmosphere. Let us set

$$A = \Sigma A_1 = N A_1, \tag{15}$$

$$m = \Sigma m_1 = N m_1, \tag{16}$$

where A_1 and m_1 are the effective area and mass of the individual particle and N is their total number. The observed deceleration will be:

$$\dot{v} = - \frac{\Gamma A_1 \rho v^2}{m_1} \, . \tag{17}$$

The amount of mass lost will be N times that lost by a single particle, or:

$$\Sigma \dot{m}_1 = \dot{m} = - \frac{\Lambda}{2\Gamma\zeta} N A_1 \rho v^3 . \tag{18}$$

Dividing (18) by (17) we obtain

$$\frac{\dot{m}}{N m_1 v \dot{v}} = \frac{\Lambda}{2\Gamma\zeta} = \sigma . \tag{19}$$

But $N m_1 = m$ is just the value which we would obtain by integrating the intensity (equation 10) and would use in computing σ. We are left with the result:

$$\sigma = \frac{\dot{m}}{m v \dot{v}} \, , \tag{20}$$

which represents no change from the case of a single body. From the observed value of σ, we could not detect the character of the meteor model proposed here. It should be clear, though, that such an object would be over-luminous, of short duration and would possess too great a deceleration.

As our second model, we assume the meteoroid to be essentially a source of particles only. In this instance we maintain a high area-to-mass ratio by a continuous fragmentation of particles but we do not greatly affect the deceleration. In the extreme case, the deceleration is a

function of the main meteoroid body and the mass loss is a
function of a large number of smaller particles. The main
body still suffers collisions with the air molecules - and
is decelerated by them - but its surface area is too small,
in comparison to the combined area of the particles, to
produce an appreciable amount of vaporized material. The
small particles, on the other hand, produce most of their
light shortly after leaving the meteoroid, but they are
continually replaced by new fragments. Denoting by A_p and
m_p the total effective area and the mass of the fragmented
particles, and by A_b and m_b the area and mass of the meteor
body which is the source of these particles, we may write
for the general case:

$$\dot{m}_p = - \frac{\Lambda}{2\zeta} A_p \rho v^3, \qquad (21)$$

$$\dot{m}_b = - \frac{\Lambda}{2\zeta} A_b \rho v^3, \qquad (22)$$

where $\dot{m}_b$ represents the mass lost by the meteoroid by direct
vaporization. Then, the total mass per second introduced
into the atmosphere in the form of vaporized material is:

$$\dot{m}_p + \dot{m}_b = \dot{m} = - \frac{\Lambda}{2\zeta} \rho v^3 \, (A_p + A_b). \qquad (23)$$

The observed deceleration will be:

$$\dot{v}_b = - \frac{\Gamma A_b \rho v^2}{m_b} . \qquad (24)$$

Dividing (23) by (24), we obtain

$$\sigma_{obs} = \frac{\dot{m}}{m_b v \dot{v}_b} = \frac{\Lambda}{2\Gamma\zeta} (1 + \frac{A_p}{A_b}) = \sigma (1 + \frac{A_p}{A_b}). \qquad (25)$$

Consequently, when we compute the quantity on the left side of equation (25), we do not obtain a number which is solely a function of those physical constants that describe the behavior of meteors in the atmosphere. Instead, we determine some number which will be larger (unless $A_p = 0$) than $\sigma = \frac{\Lambda}{2\Gamma\zeta}$.

We must mention also another complicating factor which will alter equation (25). We must question our observed value of m_b. There will always be a certain number of fragments which have left the major body but have not yet vaporized. These particles will not be observed as "mass lost" until some later instant when the vaporization has occurred. Consequently, we will always be overestimating the mass, m_b, of the parent body by the amount of mass contained in these fragments. Similarly, we will be overestimating the area, A_b, of the parent body. The deceleration, $\dot{v}_b$, is a directly measured quantity and is related to the actual mass of the parent body, not to the mass we derive by integrating the light curve. Therefore, we have, in effect, divided apples by bananas in equation (24). The same is true for the factor A_b in equations (22) and (23). Here we should have used a smaller area to determine the mass loss by direct vaporization from the parent body. To adjust these quantities to their correct values, let us set:

$$k\, m_b = m_b' \text{ where } k < 1, \tag{26}$$

and

$$k_A\, A_b = A_b' \text{ where } k_A < 1, \tag{27}$$

and where the primes indicate the correct values. If we assume that the parent body has the same shape (see equation 2) before and after it has fragmented the particles, we can write

$$k_A = (k)^{2/3} \tag{28}$$

and equation (27) becomes:

$$(k)^{2/3} A_b = A_b'. \tag{29}$$

We may now rewrite equation (25) in its proper form as:

$$\frac{\overset{\circ}{m}}{k m_b v \overset{\circ}{v}_b} = \sigma \left(1 + \frac{A_p}{(k)^{2/3} A_b}\right) = \sigma'_{obs}, \tag{30}$$

or, multiplying equation (30) by k,

$$\sigma_{obs} = \sigma \left(1 + \frac{A_p}{(k)^{2/3} A_b}\right) k = k\, \sigma'_{obs}. \tag{31}$$

For a numerical example, we may rewrite this equation for the special case where: (1) all fragments and the parent body are spherical and have the same density; and (2) all fragments are of the same mass, m_1. Then the total mass of the particles is:

$$m_b \, (1 - k) = \sum m_i = N \, m_i, \tag{32}$$

where $\underline{N}$ is the number of such particles.

The radius of each particle will be:

$$r_i = \left(\frac{m_i}{4/3\pi\delta_m}\right)^{1/3} = \left(\frac{3m_b(1-k)}{4\pi\delta_m \, N}\right)^{1/3}. \tag{33}$$

The effective area of all particles is then:

$$A_p = N\pi \left(\frac{3m_b(1-k)}{4\pi\delta_m \, N}\right)^{2/3}. \tag{34}$$

Similarly, the effective area of the parent body is:

$$A_b' = \pi \left(\frac{3m_b \, k}{4\pi\delta_m}\right)^{2/3}. \tag{35}$$

Substituting these results in equation (31), we find that

$$\sigma_{obs} = \sigma\left[1 + (Nk)^{1/3} \, (1 - k)^{2/3}\right]. \tag{36}$$

To obtain an idea of the degree of fragmentation needed to explain some of the observed discrepancies of σ we have computed some combinations of k and N which give a value of $\frac{\sigma_{obs}}{\sigma} = 10$. Table 2 gives these results (computations made for 0.1 gram meteor).

Table 2

Values of k and N Necessary to Give $\frac{\sigma_{obs}}{\sigma} = 10$

for 0.1 gram meteor (See Text)

k	N	m_1 (grams)
0.90	8.1×10^4	1.2×10^{-7}
0.75	1.6×10^4	1.6×10^{-6}
0.50	5.8×10^3	8.6×10^{-5}
0.25	5.2×10^3	1.4×10^{-5}
0.10	9.0×10^3	1.0×10^{-5}

We should point out that this approach is not limited
to the case discussed above. The reader will see that it
may be easily generalized for any distribution of particle
sizes. There may be, for example, a number of parent bodies,
each of which is fragmenting. In this case, the deceleration
would apply to the largest of these. Also, the solution
may be generalized to include shapes other than spherical
or to include separate densities for the fragments and the
parent bodies. But as we shall see in Chapter IV, such
refinements can be of academic interest only -- the
observations will not be sufficiently good to determine
so many separate variables.

CHAPTER II

NEW DATA AND THE METHOD OF APPROXIMATE REDUCTIONS

A. The Super-Schmidt Meteor Cameras

The data for this thesis are derived almost entirely from double-station photographs obtained with the four Baker Super-Schmidt meteor cameras operated by the Harvard Meteor Project at Soledad Canyon and Dona Ana Stations in New Mexico and supported by contracts with the U. S. Naval Bureau of Ordnance, the Office of Naval Research and the U. S. Air Force. These instruments and their auxiliary equipment are described in some detail elsewhere (Whipple, 1951), (Carrol, McCrosky, Wells and Whipple, 1951). A schematic diagram of the optical system (Figure 1) and an enumeration here of some pertinent quantities will be sufficient to explain the reduction technique.

Table 3

Physical and Optical Properties of the
Baker Super-Schmidt Meteor Cameras

Aperture	12.25 inches
Effective Focal Length	7.94 inches
Effective Focal Ratio	0.82
Field	55°
Focal Surface	spherical section of radius 7.9 inches, chordal diameter 7.4 inches
Shutter Speed	1800 r.p.m.

ASPHERIC SURFACE

THE SUPER-SCHMIDT METEOR CAMERA
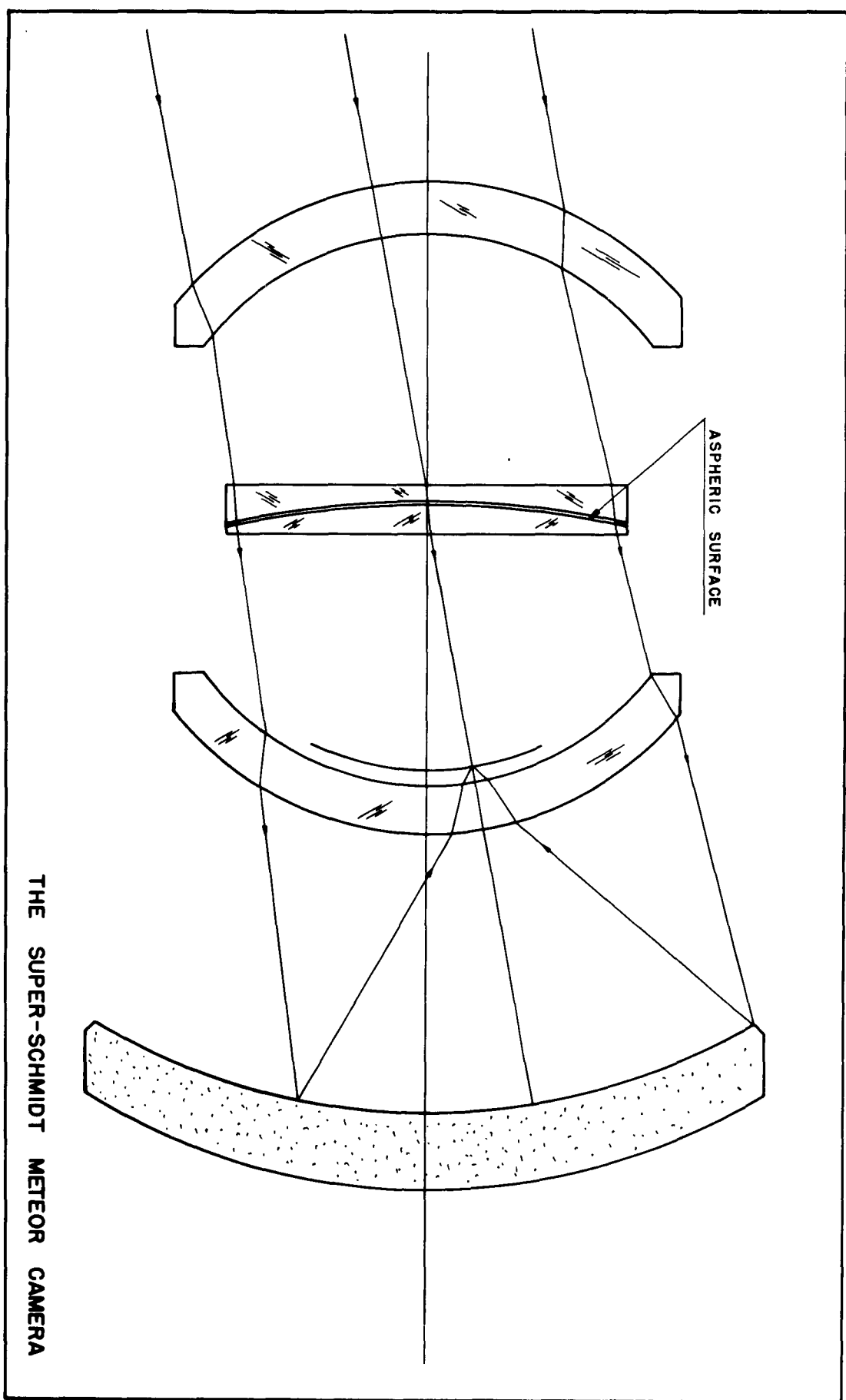
The rotating shutter lies about one-quarter of an inch outside of the focal surface. It is a spherical section concentric with the focal surface. The size and location of the shutter openings are shown in Figure 2.

The image quality is uniform over the field. Coma is detectable in brighter images but at least 50 percent of the intensity of a point source falls on a circle of 15 μ diameter. There is essentially no distortion of the spherical projection of the sky.

All photographs of meteor trails have been obtained on Eastman-Kodak X-Ray film. The film is molded, under heat and pressure, to the shape of the focal surface (Carrol et al., 1951). Although the film has not been shown to receive a permanent set to the spherical section, measures of one-year old film show little or no deviation from the original curvature. The general characteristics of the X-Ray film are similar to those of the Eastman I-O Spectroscopic emulsion. That is, it is a fast, blue sensitive emulsion with considerable graininess. Its high reciprocity failure is ideal for meteor photography, since it minimizes the density due to star and night sky light. Sky fog becomes serious with an effective exposure of more than three minutes. Since the rotating shutter excludes three-quarters of the light, exposures of 12 minutes duration are feasible with this emulsion.
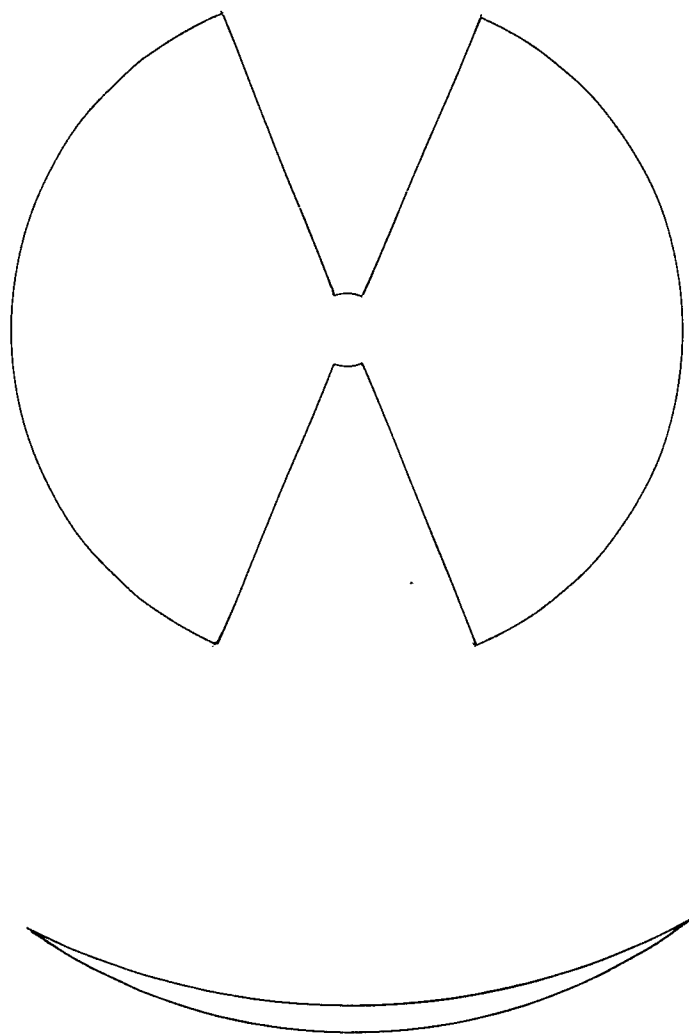
FIGURE 2

PLAN VIEW AND RADIAL SECTION
OF METEOR CAMERA SHUTTER

The exceptional effectiveness of the camera and emulsion are best described in terms of actual performance. Meteors are photographed at a rate of about one per 18 minutes of exposure. The visual magnitude of the faintest meteor images is of the same order as the limiting magnitude seen by the naked eye.

B. Meteor Heights

When the approximate reduction program was first considered, the criteria for a "satisfactory" method were rather vague. However, from the experience gained in the accurate reduction program, one could be certain that data with errors as small as 1 percent in velocities and heights could not be obtained with a reasonable expenditure of time. At the other extreme, one could question the value of statistics derived from data with mean errors of about 10 to 15 percent. With these limitations on the accuracy, a search for a sufficiently rapid method was made. To anticipate the general result of this attempt, we may state that the method to be described yields mean errors of about 5 percent. Thirty minutes is required to complete the reduction of a meteor pair. The method can be best explained if we first derive the necessary equations, next discuss separately the methods of measurements, and finally, return to the equations and estimate the magnitude of errors due to various simplifying assumptions and to errors of measurement.

The geometry of the problem can be seen in Figure 3, where R_{AB} is the distance between stations; R_A is the distance from Station A to some point on the meteor path, R_B is the distance from Station B to the same point in space. This point, on either meteor trail, will be referred to as a common point (C). The orientation in space of the triangle (A, B, C) is described by the declination (δ) and the hour angle (t) coordinates. (See Figure 3). R_{AB}, δ_{AB} and t_{AB} are constants of the stations. The hour angle and declination represent the direction of the Dona Ana Station as seen from the Soledad Station. The stations were surveyed by the White Sands Proving Grounds. Their results and the station constants are given in Table 4.

Table 4

Constants for New Mexico Stations

	Soledad Canyon	Dona Ana
Altitude (α)	1.57	1.41
Latitude	32° 18' 06"	32° 30' 22"
Longitude	106° 36' 38"	106° 47' 58"
R_{AB}	28.80 km	
t_{AB}	+124°.7	
δ_{AB}	+ 41°.5	

From the spherical triangle, (Pole, P_{AB}, P_1), we solve for γ_1, the angle between the direction to the meteor and the

direction of the line joining the stations:

$$\cos \gamma_1 = \sin \delta_1 \sin \delta_{AB} + \cos \delta_1 \cos \delta_{AB} \cos(t_{AB} - t_1). \quad (37)$$

The subscript 1 refers to either Station A or Station B. With γ_A and γ_B determined, the values of the ranges, R_A and R_B are found from:

$$R_1 = R_{AB} \frac{\sin \gamma_j}{\sin(\gamma_B - \gamma_A)}, \quad i \neq j. \quad (38)$$

The height of the common point above ground, assuming a flat earth, is then:

$$h_1 = R_1 \cos Z_1, \quad (39)$$

where Z is the zenith distance of the common point and cos Z is given by the equation:

$$\cos Z_1 = \sin \emptyset \sin \delta_1 + \cos \emptyset \cos \delta_1 \cos t_1. \quad (40)$$

We have used for the latitude, $\emptyset$, the average value of the two stations.

Clearly the same point in space can be described by only one height, and thus $h_A \equiv h_B$. This comparison gives the first check on the computations.

The height above sea level, H, is found by assuming h to be measured from an elevation equal to the mean elevation of the two stations. In kilometers:

$$H = h + \Delta h$$
$$= h + 1.5. \quad (41)$$

Solutions for equations (37) and (38) were prepared in graphic form in order to eliminate the tedious and time-consuming task of directly forming such solutions many thousands of times.

Since both γ and cos Z are functions of δ_1 and t_1, a solution for cos Z was also prepared and superimposed on the chart for γ. These charts will not be reproduced here. They are applicable only to the data acquired at the Soledad Canyon and Dona Ana Stations, and therefore are not of great interest. Table 5 summarizes the information obtained from these graphs and from another to be discussed later.

Table 5

Description of Graphs Utilized in
the Approximate Reductions

Graph	Enter with	Read	Accuracy
Ia	$-10° \leq \delta_1 \leq 90°$ $-50° \leq t_1 \leq 50°$	γ_1	$0°.1$
Ib	Same	cos Z	0.01
II	$60° \leq \gamma_1 \leq 135°$ $60° \leq \gamma_2 \leq 135°$	R_1	1 km
III	Same	R_2	1 km
IV	$.50 \leq A \leq 1.00$ $0° \leq B \leq 20°$	sin r	.001
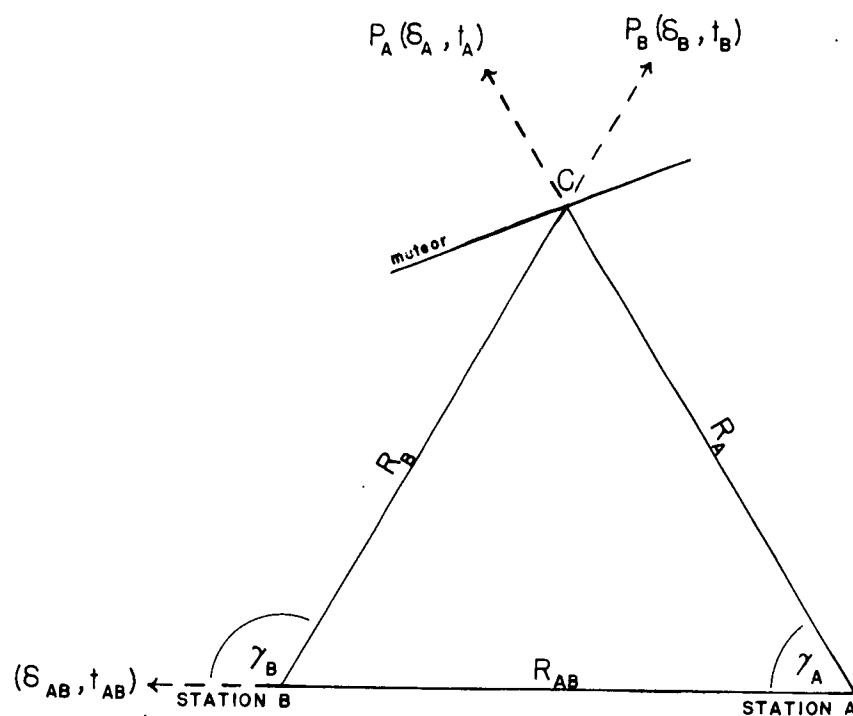
FIGURE 3

RELATIONSHIP OF GEOMETRICAL QUANTITIES
USED TO DETERMINE METEOR HEIGHTS
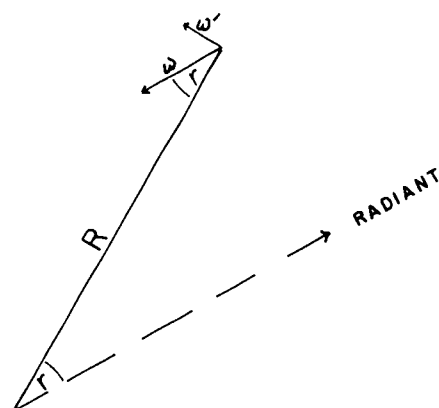
FIGURE 4

RELATIONSHIP OF GEOMETRICAL QUANTITIES
USED TO DETERMINE METEOR VELOCITIES

C. Velocities and Radiants

The meteor trail is interrupted every 1/60 sec by one
of the occulting sections of the rotating shutter. These
breaks in the trail allow one to measure the apparent angular
velocity of the meteor at some point along its trajectory.
This measure is referred to as the apparent angular velocity
since only the component normal to the line of sight is
measured. In general, such measures are made on both
photographs of the meteor at the position of the common
points.

Figure 4 shows the relationships between the apparent
angular velocity, ω'; the angular velocity, ω; and the radiant.
From this diagram we see that:

$$\omega_1 = \frac{\omega_1'}{\sin r_1} , \tag{42}$$

where r_1 is the angular distance from the radiant to the
common point. The space velocity, v, is then given by the
equation

$$v_1 = \frac{\omega_1' \, R_1}{\sin r_1} , \tag{43}$$

where R_1 is the range found in the solution for heights.
As in the case of the heights, the velocities obtained from
the two photographs should agree.

For computing purposes, equation (43) is written as:

$$v_1 = \frac{.314\ R_1}{\sin\ r_1}\left(\frac{\text{Distance}}{\text{Break}}\right), \tag{44}$$

where the quantity $\left(\frac{\text{Distance}}{\text{Break}}\right)$ is the distance between dashes
on the film in units of $1/24"$, the units of the measuring
engine we employed.

For equation (44) to be applicable, we must have
determined the position of the radiant. When the two
meteor trails intersect at a small angle, Q, it is difficult
to find an accurate radiant point. In such cases another
approach to determine the velocity is desirable. From
equation (43) we have:

$$v_A = v_B = \frac{\omega_A'\ R_A}{\sin\ r_A} = \frac{\omega_B'\ R_B}{\sin\ r_B}, \tag{45}$$

or

$$\frac{\sin\ r_A}{\sin\ r_B} = \frac{\omega_A'\ R_A}{\omega_B'\ R_B} \equiv A, \text{ by definition.} \tag{46}$$

If the apparent angular velocity is measurable on both trails
of a meteor pair, A may be computed. This gives one relation-
ship between r_A and r_B. For meteors with a small Q, it is
possible to measure $r_A - r_B$ (or $r_A + r_B$) with good accuracy.
That this is true can be most easily seen by considering
the extreme case of a meteor pair intersecting at $Q = 0°$
(or $Q = 180°$); i.e., both trails lie on the same great
circle. Then the distance between the two common points
will be exactly:

$$r_A - r_B = B \text{ (or } r_A + r_B = B), \text{ by definition.} \qquad (47)$$

The simultaneous equations (46) and (47) may be solved for $\sin r_A$ and $\sin r_B$. This solution was prepared in graphic form (see Table 5, Graph IV). With these values of r_1, v is found from (44). We have called velocities determined in such a fashion "indirect velocities" as distinct from the velocities obtained from meteors where a direct measure of the radiant is possible (direct velocities). It will be noted from equation (45) that we have forced the indirect velocities determined from each trail to agree. This comparison offers a check on the computations.

The position of the radiant may be obtained by finding the intersection of two small circles of radii of r_A and r_B with centers at P_A and P_B, respectively. In general such circles will intersect twice, but a quick inspection of the trails is sufficient to distinguish the spurious radiant point.

D. The Reduction Procedure

In this section we shall carry through the complete reduction of an imaginary meteor pair. Our purpose is not primarily one of instruction in technique, but to present, in logical sequence, the various difficulties and approximations that are present so that the reader may acquire a realization of the limitations of the method.

A separate computing form is used for each meteor.
Table 6 is such a form. Certain data necessary for each
meteor are copied from the card catalogue maintained for
all Harvard Meteors. These include:

a) meteor serial number for each trail.

b) camera designation (SS, ST, SK, SL) and
plate number for each film.

c) region of the plate center, given by δ and α.

d) astronomical date of the exposure.

e) time of meteor occurrence, to .01 minute if
the meteor was observed visually; or the
mean time of the exposure if no visual
observation was available.

The local sidereal time, in degrees, of the nearest
midnight $(L\theta_o)$ is obtained for the date. To this is added
a correction to obtain the local sidereal time $(L\theta_1)$ of the
meteor instant.

The preceding section makes it clear that the entire
method depends heavily on our ability to locate on each film
a point on the meteor trails that represents the same point
in space, the common point. If the meteor shows a burst or
some other discontinuity in the light curve, a common point
is obvious. However, the faint meteors, with which we are
primarily concerned here, usually have smooth light curves.
In these cases a more subtle technique is necessary. The

( )

Meteor		—		—
Plate	S	—	S	—
Region				
α, δ				
Date, Lθ₀	.		—	—
MST, Lθ₁				—
Star Pos.				
No.				
t				
δ				
Direction		—		—
Magnitude				

Com'n p'nt	n₁		n₂	
	SC	DA	SC	DA
Quality				
n				
δ				
t				
cos Z				
γ				
h				
H				
R				
Projec't				
Dis't/Brk	/	/	/	/
$r_{SO}-r_{DA}$ ~~$V_{SO}-V_{DA}$~~				
A				
sin r				
Velocity				
Radiant				
Q				
t, δ, α	.	.		
Shower				
cos Z_rad				
Wake				
Start: n, H				
End: n, H				

Accurate reduction data in red.

Table 6
Computing Form for Approximate
Reduction Method

number of dashes visible on each trail is counted and, if it
is the same, we assume that dashes with the same ordinal
number are common points.

Such an assumption fails in three minor respects.
Firstly, the shutters are not synchronized, i.e., we do not
know the orientation of one shutter with respect to the other
at any given instant. Consequently the common point can be
in error by as much as half the distance between dashes.
Secondly, the focal plane shutter interrupts the same
position of the film at constant time intervals. The rate
at which the meteor is interrupted depends on its direction
of motion and its apparent velocity on the film. In the
extreme case of a meteor trail passing through the film
center, an error of one dash can be made. But since the two
trails of a meteor pair are usually similar in their
direction of travel on the film, and since their apparent
velocities on the film are small compared to the shutter
velocity, the error will generally be only a small fraction
of a dash. Thirdly, in assuming that breaks with the same
ordinal number are common points, we assume that both cameras
have photographed the meteor to the same limiting absolute
magnitude or, alternatively, that the differential
distance correction from the beginning to the end of the
meteor is small or the same for both trails. Since most of
our trails are short, the differential distance correction
is small.

We can conclude that the common points chosen on trails showing the same number of breaks will be accurate to within one dash. However, the two cameras often do not record the same number of breaks for the following reasons:

a) The sensitivities of the cameras are not equal. With increasing experience in figuring the correcting plate, the manufacturer has been able to improve the quality of each succeeding camera. The effect is most noticeable when comparing trails obtained on the first (SS) and second (ST) Super-Schmidts.

b) The apparent magnitude of the meteor as seen from the two stations may differ by several tenths of a magnitude because of distance corrections. Effects (a) and (b) often compensate one another in part since the earlier camera, at Soledad Station, is directed more nearly toward the zenith than is the mate camera at the Dona Ana Station.

c) The effective exposure time per dash is proportional to ω_i'. Thus, the trail nearer the radiant is photographed as a brighter image and the plate limit is reached at a fainter absolute magnitude.

Effects (a) and (b) combined are usually minor compared to effect (c). By noting the general shape of the meteor light curve of the brighter trail, one can obtain an acceptable common point by estimating the number of dashes that failed to be recorded at the beginning and at the end of the fainter meteor trail. In only a very few cases did the combination of the factors of effective sensitivity of the camera, and the apparent velocity of the meteor, differ so much that no acceptable common point could be found. For each common point, we record under "Quality" (Table 6), an estimate of the number of dashes by which the common point may be in error. This never exceeds 3 for an acceptable meteor and rarely exceeds 2.

To mark the common points, a small piece of Scotch Tape is placed on the reverse side of the film at the location of the trail. Ink dots placed on this tape indicate the common point. For longer meteors (20 dashes or more), two common points, (n_1 and n_2 in Table 6) are chosen in order to make a check on the entire reduction. The common point is recorded as the ordinal number of the dash, the dash nearest the radiant being called "1". The duration of the meteor is measured in terms of the total number of visible dashes, N. The beginning of the trail is specified by noting, under "Direction", the octant, as seen from the meteor, in which the radiant lies.

To measure the celestial coordinates of the common points and radiant, we utilize a transparent Plexiglass hemisphere of 8-inch radius, calibrated in hour angle and declination. The scale of these calibrations and the radius of the globe correspond to the scale and radius of the Super-Schmidt films. To read the coordinates of the common point, we need only to position the film properly on the globe. We accomplish this by choosing three or four bright stars which appear on one of the films, determining the declination and hour angle of these stars at the time of the meteor, and plotting these star positions on the globe. The film is then placed on the globe so that the star images and their plotted positions coincide. Since the regions of the two mate films overlap in an area of approximately one-quarter of the film, we can position the second film by superimposing stars in this region. The hour angle and declination of the common points are then read from the globe scales.

We determine the radiant and radiant distances, r_A and r_B, with the aid of a pair of curved rulers of 8-inch radius and 90° length, attached to one another by a hinge. They are calibrated in degrees, the pivot point of the hinge being zero degrees. When each rule lies parallel to one of the meteor trails, the zero point represents the radiant. The radiant distances are read from the rules and the coordinates of the radiant point are read from the hemisphere. The

cosine of the zenith distance of the radiant ($\cos Z_R$) is determined from Nomogram Ib.

The quantity Q is the angle of intersection of the two trails. An estimate of this quantity, accurate to about 10 percent, is made when the radiant is found. The value of this angle is not used in the reductions but it serves as a measure of quality of the directly determined radiant.

The apparent angular velocity, or distance per break, is measured on the Harvard Coast and Geodetic measuring machine. This has been equipped with a section of an 8-inch radius Plexiglass sphere for the support of the film. The spherical section is large enough to permit all measurements to be made with the optical axis perpendicular to the image when the trail occurs at the edge of the film. This reduces the focussing problem and also allows us to neglect any correction for the projection effect which would be necessary if the curved film rested on the flat carriage of the measuring engine.

The number of breaks measured depends on the apparent angular velocity of the trail. In general, we attempt to measure a distance of from 1 to 3 mm, which may represent 2 to 8 breaks. The measurements are usually made from the end of one dash to the end of another; that is, an integral number of dashes is measured. Corrections, by eye, are made for the photographic spreading of the image if the two terminal dashes of the measured trail section do not appear to be of about the same intensity. The dashes to be

measured are chosen in such a way that the common point lies
in the center of the measured section.

The trails are inspected for any wake, terminal blending
or marked abnormalities in the distribution of light over
the trail. The position and apparent magnitude of the
brightest dash may be measured. The method of meteor
photometry has been described by Jacchia (1949). The
photometry has been completed on only a limited number of
the meteors dealt with here.

This completes the measurements made on a meteor
pair. We then determine, from the equations given earlier,
$\cos Z_i$, γ_i, R_i, h_i, H, A and v_i, in that order.

To complete this outline of the method, we will add
a description of an earlier approach to the problem of
finding common points. The argument, due to Olivier (1925),
proceeds as follows: Consider the plane defined by the two
stations and a point on the meteor. The lines R_A, R_B and
R_{AB} lie in this plane which intersects the celestial sphere
on a great circle. Then the position of the meteor point as
seen from each station must lie on a great circle which
also includes the celestial position of one station as
seen from the other. Conversely, if the two meteors are
located properly on the globe, we can draw a great circle
through the point defining the direction between the
stations. Then, by the argument above, the intersections of
this great circle with the meteor trails must represent

common points. This technique was tried and discarded
as being too insensitive for most cases. In practice, we
employed a movable great circle which was attached to the
measuring globe and pivoted at the points (δ_{AB}, t_{AB}) and
$(-\delta_{AB}, t_{AB} -180°)$. When the meteor trails formed a moderately
small angle with this circle, the common points could be
varied by several dashes with only a slight shift of the
films. If the time of the meteor occurrence is lacking,
the precise position of the film on the celestial sphere is
unknown.

E. <u>Single-Station Shower Meteors and the Approximate Method</u>

The program of meteor astronomy at the Harvard College
Observatory, includes the investigation of the origin and
histories of the shower meteors by study of the distribution
of the radiants over the period of the shower (see, for
example, Wright, Jacchia and Whipple, in press). Single-
station meteors are used in a least-squares solution to
determine the radiant, if they appear to belong to the
shower; that is, if an extension of the trail passes through
(or near) the assumed radiant point for the time of the
meteor, and if visual inspection determines that the
apparent angular velocity of the meteor is reasonable for
the shower velocity and the radiant distance. A small amount
of work with the globe used in the approximate method removes

the guesswork from this visual determination. By assuming
that the meteor belongs to the shower, we can estimate a
height that corresponds to that of meteors of the shower
velocity. The apparent angular velocity (ω_1'), cos Z_1, and
the distance from the assumed radiant (r_1), are measured for
some point on the trail. From equations (39) and (43),
we have:

$$V = \frac{\omega_1' \, h_1}{\cos Z_1 \, \sin r_1} \, . \qquad (48)$$

If the meteor belongs to the shower, the measured values
should yield the shower velocity. We may be deceived
occasionally by meteors whose true radiants and velocities
are not those of the shower but combine, by chance, in
such a way that

$$(v \, \sin r_1)_{shower} = (v \, \sin r_1)_{non-shower} .$$

Such cases must be far more rare than the 10 percent of
single-station meteors which we have been able to eliminate
from those meteors thought to belong to the shower.

It is probably obvious that the usual approximate
method may also be used to eliminate those double-station
meteors that have the proper radiant but a non-shower velocity.

F. Height Errors

The problem of errors in our data reduction includes
two major questions, neither of which has yet been finally
answered. First, the velocities and radiants determined by

the direct and indirect methods are, in general, at variance
with one another. We need some quantitative criteria for
making a choice between the two results. Second, we desire
a more exact knowledge of the mean errors as a function of
the various parameters of the solution. That neither of
these desiderata have been found does not affect the results
of this thesis to any reasonable extent. All the problems
treated here are of such a nature that we need not be
concerned with whether the errors are 3 percent or twice
that amount. However, we will wish to know that the errors
are not, say, 15 percent. Our brief study of errors will
show they are not.

The final answers to these questions will be found only
after the completion of the reduction project. Eventually
we intend to acquire approximate data on 2000 meteors,
including about 300 faint meteors that have been reduced by
a more accurate method. An intercomparison of results
should supply the information we want. Comparison can now
be made with several hundred brighter meteors already reduced
by Jacchia. However, the accuracy we would obtain in
determining the radiant of these long meteors will seldom
be approached for fainter meteors. On the other hand,
common points are often more difficult to obtain on long
meteors. All in all, we do not consider bright meteors to be
comparable to faint ones with regard to our system of

measuring. A comparison of velocities obtained by accurate methods and by the present method has been made for some 25 bright meteors. Our average error in velocity was about 3 percent.

With respect to the order-of-magnitude estimate we can study the results of measuring errors of probable amounts and we may compare our results for shower meteors with their known values.

Let us begin with the errors in height introduced by our assumption that the earth is a plane surface. The correction for this was ignored as being small compared with the intrinsic errors of measurement. This is true if the meteors are in the vicinity of the zenith, as they were in all the early New Mexico photographs treated here. It is easily shown that

$$\Delta h = h - h' = \frac{R^2 - h'^2}{D}, \qquad (49)$$

where h is the computed height above the station level, h' is the true height above the station level, R is the range from meteor to station, and D is earth's diameter. With the assumption that

$$\Delta h \angle\angle 2h, \qquad (50)$$

we obtain

$$\Delta h \doteq \frac{R^2 - h^2}{D + 2h}. \qquad (51)$$

Employing equation (39), we may write

$$\Delta h \pm \frac{h^2(\sec^2 Z - 1)}{D + 2h}. \qquad (52)$$

For meteors of 100 km altitude, the correction factor reaches 0.5 kilometers at a zenith distance of $37°.7$. Essentially none of the meteors in this work exceed this value. The average zenith distance is of the order of $20°$.

If the common point is improperly chosen or measured, or if the two films are not correctly positioned on the globe, the two range lines, as defined by (δ_A, t_A) and (δ_B, t_B) will either not intersect in space or will not intersect on a point on the meteor trail. Whether the intersection occurs for any given set of measures or not, our computations still lead to a complete description of some triangle which represents, to some degree of approximation, the true triangle defined by the two stations and a point on the meteor. We are interested in knowing how good an approximation our measures probably give. To investigate this, it will be most convenient to study, in the original equations, the changes brought about by independent changes in the assumed position of the common point along the t and δ axes. Differentials of equations (37), and (40), (38) and (39) yield:

$$\left(\frac{\Delta \gamma}{\Delta \delta}\right)_t = -\frac{\cos \delta \sin \delta_{AB} + \sin \delta \cos \delta_{AB} \cos (t_{AB}-t)}{\sin \gamma}, \quad (53a)$$

$$\left(\frac{\Delta \gamma}{\Delta t'}\right)_\delta = -\frac{\cos \delta_{AB} \sin (t_{AB}-t)}{\sin \gamma}, \quad (53b)$$

$$\left(\frac{\Delta Z}{\Delta \delta}\right)_t = -\frac{\sin \emptyset \cos \delta + \cos \emptyset \sin \delta \cos t}{\sin Z}, \quad (54a)$$

$$\left(\frac{\Delta Z}{\Delta t'}\right)_\delta = \frac{\cos \emptyset \sin t}{\sin Z}, \quad (54b)$$

$$\left(\frac{\Delta R_A}{\Delta \gamma_A}\right)_{\gamma_B} = \frac{R_{AB}}{57.3}\left\{\frac{\sin \gamma_B \cos (\gamma_B-\gamma_A)}{\sin^2 (\gamma_B-\gamma_A)}\right\}, \quad (55a)$$

$$\left(\frac{\Delta R_B}{\Delta \gamma_B}\right)_{\gamma_A} = -\frac{R_{AB}}{57.3}\left\{\frac{\sin \gamma_A \cos (\gamma_B-\gamma_A)}{\sin^2 (\gamma_B-\gamma_A)}\right\}, \quad (55b)$$

$$\left(\frac{\Delta R_A}{\Delta \gamma_B}\right)_{\gamma_A} = -\frac{R_{AB}}{57.3}\left\{\frac{\sin \gamma_A}{\sin^2 (\gamma_B-\gamma_A)}\right\}, \quad (55c)$$

$$\left(\frac{\Delta R_B}{\Delta \gamma_A}\right)_{\gamma_B} = \frac{R_{AB}}{57.3}\left\{\frac{\sin (\gamma_B)}{\sin^2 (\gamma_B-\gamma_A)}\right\}, \quad (55d)$$

$$\left(\frac{\Delta h}{\Delta \delta}\right)_t = \cos Z \left(\frac{\Delta R}{\Delta \delta}\right)_t - \frac{R}{57.3}\left[\sin Z \left(\frac{\Delta Z}{\Delta \delta}\right)_t\right], \quad (56a)$$

$$\left(\frac{\Delta h_i}{\Delta \delta_j}\right)_{t_j} = \cos Z_i \left(\frac{\Delta R_i}{\Delta \delta_j}\right)_{t_j}, \quad i \neq j, \quad (56b)$$

$$\left(\frac{\Delta h}{\Delta t'}\right)_\delta = \cos Z \left(\frac{\Delta R}{\Delta t'}\right)_\delta - \frac{R}{57.3}\left[\sin Z \left(\frac{\Delta Z}{\Delta t'}\right)_\delta\right] \quad \text{and} \quad (56c)$$

$$\left(\frac{\Delta h_i}{\Delta t_j'}\right)_{\delta_j} = \cos Z \left(\frac{\Delta R_i}{\Delta t_j'}\right)_{\delta_j}, \quad i \neq j. \tag{56d}$$

The subscripts on the differentials refer to those variables held constant during the differentiation. The differential angles are all expressed in degrees of arc, having been converted from radian and from degrees of hour angle when necessary. The parameter

$$\Delta t' = \Delta t \cos \delta. \tag{57}$$

We will discuss the errors involved in one particular case. Computations for other cases show that the total errors will be similar in other parts of the sky where meteors have been photographed. As our example, we will use a meteor with the common point coordinates given in Table 7. The remaining values in the table were computed from the equations previously given. The accuracy, of course, exceeds that which may be obtained from reading the nomograms and also exceeds the amount commensurate with the ultimate accuracy of the measures ($0°.1$).

It is a bit difficult to estimate a reasonable amount for the errors in the common point, positioning, or measuring which combine to give the total errors, $\Delta \delta$ and Δt.

Table 7

Differential Errors Produced by an Error in the Common Points

		Station A	Station B
δ		+27.6	+13.9
t		+13.5	-0.4
γ		86.2	105.0
R	(km)	86.31	89.16
cos Z		.976	.948
h	(km)	84.2	84.5
H	"	85.8	85.9
$\left(\dfrac{\Delta R_1}{\Delta \gamma_1}\right)_{\gamma_j}$	$\dfrac{\text{km}}{\text{degree}}$	+4.43	-4.57
$\left(\dfrac{\Delta R_1}{m\gamma_j}\right)_{\gamma_1}$	"	-4.83	+4.68
$\left(\dfrac{\Delta \gamma}{\Delta \delta}\right)_t$	$\dfrac{\text{degree}}{\text{degree}}$	-0.714	-0.773
$\left(\dfrac{\Delta Z}{\Delta \delta}\right)_t$	"	-0.433	-1.000
$\left(\dfrac{\Delta R_1}{\Delta \delta_1}\right)_{t_1}$	$\dfrac{\text{km}}{\text{degree}}$	-3.16	+3.53
$\left(\dfrac{\Delta R_1}{\Delta \delta_j}\right)_{t_j}$	"	+3.73	-3.34
$\left(\dfrac{\Delta h_1}{\Delta \delta_1}\right)_{t_1}$	"	-2.94	+3.84
$\left(\dfrac{\Delta h_1}{\Delta \delta_j}\right)_{t_j}$	"	+3.64	-3.17

Table 7 (continued)

			Station A	Station B
$\left(\dfrac{\Delta\gamma_1}{\Delta t'_1}\right)_{\delta_1}$	$\dfrac{\text{degree}}{\text{degree}}$		-0.700	-0.634
$\left(\dfrac{\Delta Z_1}{\Delta t'_1}\right)_{\delta_1}$	"		+0.904	-0.019
$\left(\dfrac{\Delta R}{\Delta t'_1}\right)_{\delta_1}$	$\dfrac{\text{km}}{\text{degree}}$		-3.10	+2.90
$\left(\dfrac{\Delta R_1}{\Delta t'_j}\right)_{\delta_j}$	"		+3.06	-3.28
$\left(\dfrac{\Delta h_1}{\Delta t'_1}\right)_{\delta_1}$	"		-3.12	+2.72
$\left(\dfrac{\Delta h_1}{\Delta t'_j}\right)_{\delta_j}$	"		+2.99	-3.11

The error involved in reading the globe scale should not exceed $0°.2$. For fast meteors with a high apparent angular velocity and with a common point of only moderate quality, say 2, the common-point error would be about $1°$. We believe this to be considerably greater, perhaps by a factor of 2, than the common-point error for the average meteor. Positioning errors can occur in two ways. First, the two films may not be properly superimposed. Because the globe is not perfectly spherical and because its mean radius is not exactly that of the films, we can not always superimpose the entire star field common to both films. The attempt is always made to carry out the superposition in the vicinity of the meteors and an error of about $0°.5$ would probably be large. The second positioning error, resulting from an unknown time of the meteor occurrence, is a special case and will be treated separately.

From the preceding extreme figures, we may estimate that the average error, in t_1 or δ_1, will almost certainly not exceed $1°$. It is unfortunate that this figure cannot be verified by more rigorous methods than those used. However, another check on our errors, to follow later, will supply additional information tending to confirm this as being an extreme value.

Let us assume that the common point at Station B has been properly located, positioned and measured, and that, for any of the aforementioned reasons, a $1°.0$ error exists

in the measures of the common point at Station A. The percentage errors for this case, computed from the quantities in Table 7, are given in Table 8.

Table 8

Errors Resulting from a $1°.0$ Error in the Common Point

Percentage Error in:	$\Delta\delta_A = 1°.0$	$\Delta t'_A = 1°.0$
R_A	3.7%	3.6%
R_B	3.7	3.7
h_A	3.5	3.7
h_B	3.8	3.7

The similarity of values within either column should be expected. The similarity between corresponding values of the two columns is the result of chance and indicates that the maximum error for the meteor will occur for departures in a direction roughly half way between the directions of the δ and the t axes.

When the instant of the meteor is unknown, we choose the time of the middle of the exposure for reduction purposes. Thus, with 12-minute exposures our maximum error is $\Delta t = 6$ mins $= 1°.5$. However, in this case the common points do not suffer a shift relative to one another and the resulting errors in the ranges will be the algebraic sums of the errors caused by the displacement of both common

points. Since these are of opposite sign and of about the
same magnitude (see Table 7), the final errors will be small.
Table 9 shows the percentage errors resulting from a $1°.5$
shift in t of both films.

Table 9

Errors Resulting from a Displacement of $\Delta t = 1°.5$ of Both Films

Quantity	R_1	R_2	h_1	h_2
Error (km)	+0.34	-0.14	+0.20	-0.17
Percentage Error	0.4	0.2	0.2	0.2

We can see that the timing error will be negligible even in
those cases where the maximum possible error results from a
displacement along the t-axis.

G. Velocity Errors

Errors in velocity may result from errors in any of
the measures. Errors in the apparent angular velocity, ω_1',
are probably small compared to any other type and we will
neglect these. From differentials of equation (43) we
see that the percentage errors due to range and radiant
errors are, respectively:

$$\left(\frac{\Delta v}{v}\right)_{\omega'} = \frac{\Delta R}{R}, \text{ and} \tag{58a}$$

$$\left(\frac{\Delta v}{v}\right)_{\omega', R} = - \cot r \, \Delta r. \tag{58b}$$

Thus the error in velocity cannot be less than the range error, which we found to be about 4 percent with the assumption of a common point error of 1°.0. The function Δr is itself a function of r as one can understand by visualizing the extreme cases when the meteor appears <u>at</u> the radiant ($r = 0°$, $\Delta r = 0°$), and when the meteor appears at a great distance from the radiant (say, $r = 90°$, $\Delta r = ? \neq 0°$). We might estimate this unknown Δr to be of the order of $5°$ or $10°$ in the worst cases. We may say that certainly Δr varies less rapidly than tan r. This leads to the apparently contradictory result that, in general, meteors must have a badly determined radiant to allow us to produce an accurate velocity. However, another independent error in r, that imposed by our scale reading accuracy, $0°.2$, weighs more heavily against meteors of small r. These two errors may combine in such a way that meteors at some intermediate r give the best velocities.

We have no method of determining a satisfactory relationship between r and Δr and we must therefore approach this problem from another side. Among the meteors reduced, there are 36 Orionid and 45 Geminid shower meteors for which we know velocities. These groups will determine our velocities errors. Furthermore, since most meteors in these showers were reduced by both the direct and indirect methods, we can find some estimate of a criterion for choosing between the results of the two methods.

In general, the direct velocities derived from the two films of a given meteor do not agree with one another to within several percent. However, in some examples, the radiant distance of one common point greatly exceeds that of the mate plate and in these instances, the velocity derived from the more distant trail was used or weighted more heavily in the average. Average velocities, mean errors and percentage errors were found for both sets of shower meteors for the following cases:

(a) Direct velocity used for all meteors.

(b) Indirect velocity used for all meteors.

(c) Indirect velocities used when $|B| \geq 10°.0$, direct when $|B| < 10°.0$.

(d) Same as (c), with division made at $|B| = 9°.0$.

(e) Same as (c), with division made at $|B| = 8°.0$.

Table 10 gives the average values, mean deviations and percentage errors for each of these velocity criteria and for both groups of shower meteors. The letters refer to the outline above.

Table 10

Mean Values and Errors of Shower Meteor Velocities

(For description, see text)

	Number of Meteors	Number of indirect determinations used	$V\left(\frac{km}{sec}\right)$	$\sigma\left(\frac{km}{sec}\right)$	% error
Geminids					
(a)	44	0	35.7	1.42	4.0%
(b)	38	38	35.7	1.74	4.9
(c)	45	16	36.3	0.92	2.5
(d)	45	21	36.1	1.05	2.9
(e)	45	26	36.0	1.13	3.1
Orionids					
(a)	34	0	68.3	3.01	4.4%
(b)	34	34	67.2	2.52	3.8
(c)	36	18	68.2	2.59	3.8
(d)	36	24	67.7	2.17	3.2
(e)	36	28	67.6	2.05	3.0

We should qualify these data before discussing the
results. First, the Geminids were somewhat brighter meteors
than normal and, hence, easier to measure. Furthermore, the
radiant of this shower is not far distant from α Geminii, a
star that appears on most of the Geminid meteor photographs.
Since these meteors were reduced specifically to check for
errors, it was necessary for the measurer to "forget" the
position of the radiant for each measure, a difficult task
with a radiant so clearly marked. Still, we believe this
was accomplished.

In the case of Orionids, the situation is quite different.
The radiant was not present on the region being photographed
and, more important, we did not realize we were reducing

shower meteors until after the measures had been completed. Also, these meteors did not produce such bright trails as the Geminids. Perhaps, then, the Orionids should be regarded as giving the best test, although, as can be seen in Table 10, the errors for both showers are comparable.

In regard to the indirectly determined velocities, our measured quantities are A and B as defined by equations (46) and (47). It may easily be shown that if the radiant is properly chosen and there are no measuring errors, then

$$\Delta r_A = \Delta r_B = \frac{(\Delta A + \Delta B) \sin^2 r_+}{\sin B} \tag{59}$$

where r_+, is the angle from the radiant to the common point of the trail most distant from the radiant. A poorly determined common point has little effect on A, since this quantity is determined from a ratio of the ranges, R_i/R_j. We have already seen that a reasonable error in the common point results in comparable changes, of the same sign, in the two ranges. We may write:

$$A \sim \frac{R_A}{R_B}. \tag{60}$$

Differentiating this equation, we obtain

$$\Delta A = \frac{R_B \, \Delta R_A - R_A \, \Delta R_B}{R_B^2}. \tag{61}$$

Thus, the errors in the range tend to compensate one another in the determination of A. However, since we must still apply the velocity equation (43) in its original form after determining r_1, any error in range will affect the velocity in the usual fashion.

One can see that an error in the common point will directly effect B which is essentially the distance between common points. It is also clear from the $\frac{1}{\sin B}$ factor in equation (59) that the indirect method will be more powerful when $|B|$ is sufficiently large. From the shower meteors we can obtain an idea of how large.

Table 10 indicates that the deviation from the mean velocities of the showers is of the order of 3 to 4 percent, but we have yet to show that these mean velocities actually correspond to those expected for these showers. Our velocities are those at some point in the atmosphere, uncorrected for deceleration and therefore somewhat lower than the usually quoted velocity outside the atmosphere. In general, we choose common points as near the beginning of the trail as possible to minimize the deceleration correction. From Orionid and Geminid meteors reduced by Jacchia, we have obtained the velocities at the beginning point of the meteor. (v_o). These results, as well as Jacchia's values for the no-atmosphere velocity (v_∞) are given in Table 11. They are compared with the average velocity we obtained for the method which yielded the smallest σ in Table 10

Table 11

Average Velocities of Shower Meteors Obtained

by Accurate Reductions

(By Jacchia)

	No. Meteors	v_∞	v_0	v_{REM}
Geminids	17	36.6	36.3	36.3
Orionids	7	67.5	67.4	67.6

The agreement is excellent and there is no evidence for a systematic error with velocity. We may conclude that our velocity errors, for these cases, are about 3 percent, and that the optimum minimum value of $|B|$ for the indirect reductions is about $8°$ to $10°$. It seems unlikely that measures on somewhat shorter and fainter non-shower meteors would yield errors that exceed 5 percent. When this result is compared with the errors expected for ranges and heights, we see that we must have over-estimated the probable error in the common point, for as was pointed out earlier, the velocity error cannot be less than the range error, which was of the order of 4 percent on the assumption of a $1°.0$ error in common point.

There still remains the possibility that in selecting the shower meteors, we passed over some cases which were so badly determined that they were unrecognizable as members of the shower. A study of the frequency diagram of the

velocities of the individual meteors makes such a hypothesis
unlikely if, on the basis of such a diagram, one is willing
to grant that the scatter may be represented to a fair degree
of approximation by the usual error curve. We have reproduced
in Figure 5 the frequency diagram for the directly determined
velocities of our Geminid meteors.

Figure 5

VELOCITY DISTRIBUTION OF GEMINID SHOWER METEORS, APPROXIMATE REDUCTIONS
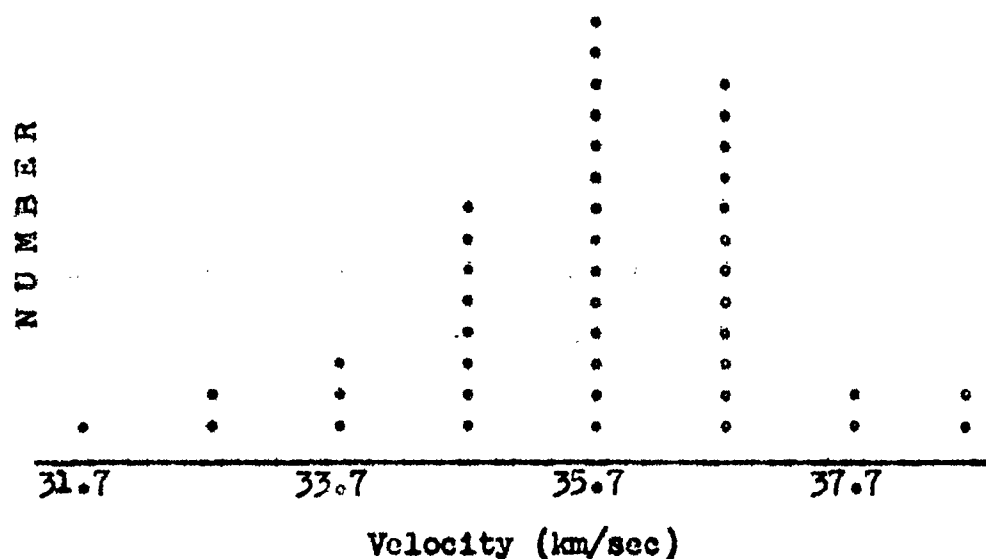
H. Some Specific Results of the Approximate Reduction Method

In selecting meteors for approximate reductions, we inspected every meteor film, in chronological order, to determine whether it was possible to make a reduction. We discarded as few meteors as possible, and would have preferred to exclude no meteors, so that the over-all statistics would be unassailable. However, some individual cases clearly would have yielded results of very poor quality. About 15 percent of the meteors were in this category, and rejected for one of the following reasons:

> (a) The meteor was too faint or too short for the radiant to be determined.
>
> (b) The difference in image quality (focus or fog) of the mate films was such that no satisfactory common point could be found.

A further fifteen percent of the meteors were also discarded because their geometry or positions made reductions impossible or difficult. These included:

> (c) Meteors so close to the radiant on <u>both</u> films that the photographic spreading of the image obscured the breaks.
>
> (d) Meteors that appeared on the film only in part and, as a consequence, could not yield a satisfactory common point. Not all such partial meteors were excluded, however, since in many cases a good estimate of a common

point could be made.

In addition, another fifteen percent of the meteors photographed were not available for reduction at the time of this study. They include:

(e) Meteors being reduced in the accurate reduction program. These, in general, are brighter than those we have treated. Their exclusion is responsible for the homogeneity, with respect to brightness, of our meteors.

(f) Other meteors occurring on the films included in (e). These, we suppose, are a random selection in all respects.

Of the remaining 55 percent which we reduced, we later discarded from the statistics a very small fraction of a percent, because large discrepancies in the final results indicated that a solution was too difficult.

At present (November, 1955), data are available for about 1600 meteors, photographed from the beginning of the double-station Super-Schmidt program, February, 1952, through February, 1954. Present plans call for a total of at least 2000 meteors photographed over a period of at least two years.

The data we wish to present here do not include all that are available. The results quoted in the remainder of this thesis are based on all the reductions that had been

completed at the time the particular analysis was made. This
will explain the varying number of meteors we include in
attacking the several aspects of this study.

To begin with, we shall mention briefly the distribution
of meteor velocities. Although we wish to divorce this
aspect of the data from the general subject of the thesis
and to treat it separately in a later paper, we shall need
to refer to the distribution when discussing fragmentation
phenomena. Table 12 summarizes the data on the first
1069 meteors to be reduced. Included are meteors occurring
between February 1952 and June 1953. For comparison we
have also listed the early information, compiled by Whipple
(1954), obtained from the small camera meteors. His
velocities are those at the top of the atmosphere, V_∞, and
ours at the measured common point nearest the beginning of
the trail. The slight correction for deceleration necessary
to make the two groups strictly comparable is very small
compared to the 10 km/sec sub-groups we have chosen. We
have also listed the distribution of all meteors, expecting
the Perseid, Orionid, and Geminid showers, which add an
appreciable number to either the present or to Whipple's
total. Whipple lists a total of only 51 sporadic meteors
and consequently the elimination of all shower meteors leaves
few for comparison.

Table 12

Velocity Distribution of 1069 Super-Schmidt Meteors

Compared with the Distribution of 144 Small Camera Meteors

(See Text for Classifications)

v km/sec	Percent of Total for Cases:				
10-15	13.7 %	14.8 %	3.5 %	4.5 %	3.9 %
15-20	16.5	17.8	6.2	8.1	15.7
10-20	30.2	32.6	9.7	12.6	19.6
20-30	22.7	24.6	24.3	31.5	27.5
30-40	21.0	18.2	30.6	22.5	15.7
40-50	6.5	7.1	6.9	9.0	3.9
50-60	9.8	5.2	5.6	5.4	9.8
> 60	14.8	12.3	22.9	18.9	23.5

The five categories of meteors listed in the table include the following:

> (a) 1069 Super-Schmidts, representing all those occurring between February, 1952, and June, 1953, and reduced by approximate means.

> (b) 988 meteors remaining from (a) after the exclusion of all meteors in three major showers (45 Geminids, 36 Orionids, 0 Perseids).

> (c) 144 small camera meteors by Whipple (1954).

> (d) 111 meteors remaining from (c) after the exclusion of all meteors in three major showers (19 Geminids, 2 Orionids, 12 Perseids).

> (e) Those meteors (51) in (c) that are sporadic.

Regardless of which categories of meteors we compare, we see that the older data rather badly underestimated (or we have overestimated) the number of meteors in the lowest velocity group. It may be that the explanation lies in the choice of meteors accepted for accurate reduction. Meteors of low apparent velocity may have the shutter breaks greatly obscured by photographic diffusion of the dash image, so that the meteors are difficult or impossible to measure. Such cases would be selectively rejected, leaving a preponderance of faster meteors.

Statistics concerning phenomena apparently caused by fragmentation of the meteor are available for 585 cases, all the meteors occurring between February and December, 1952. For each of these meteors we have recorded the presence and position of wake and terminally blended dashes. The wake, in the best examples, is seen as a trail of steadily decreasing luminosity extending from a dash towards the direction of the radiant. When the wake is strong, the image due to both dash and wake may assume a tear-drop shape. In more usual cases one can only notice that the dash lacks symmetry in the direction of the meteor's motion. For faint photographic meteors, one cannot be more explicit in describing the appearance of wake.

Terminal blending, in the strict sense, is a term that should be reserved to describe those dashes that do not necessarily show an asymmetry but are longer than the

expected one-fourth of a shutter cycle. Often the final images will be very faint but will clearly be more diffuse than some earlier images. We cannot always decide whether such an image should be designated as wake or as terminal blending. We generally classified such cases as blending. Although this represents a consistent approach, the result has probably been to overweight the occurrence of blending by an appreciable amount. Good examples of wake are certainly more common than good examples of terminal blending and perhaps one should expect the same to be true for the poorer examples. By expressing some doubt concerning the number of meteors displaying each of these characteristics, we do not wish to imply a question as to whether any of these meteors displayed one of the fragmentation phenomena.

In 1954 we made a preliminary study of the correlation of the visible effects of fragmentation and velocity, on the basis of some 50 faint meteors. The analysis of the 585 meteors confirms the conclusion that the existence of wake and of terminal blending are both a function of velocity. Table 13 lists the results.

Table 13

Percentage of Meteors in Various Velocity Groups that

Display Some Visible Effects of Fragmentation

v (km/sec)	Wake	Terminal Blending	Wake and Terminal Blending	Wake and/or Terminal Blending
10-15	32%	79%	23%	89%
15-20	41	53	25	69
10-20	37	63	24	77
20-30	39	30	11	57
30-40	29	32	16	44
40-50	25	9	3	31
50-60	10	8	3	15
>60	12	3	1	14
ALL	28%	30%	12%	45%

For the reasons given above, the final column of Table 13
should be considered to be the best set of data; it gives the
percentage of meteors in the given velocity groups that show
wake or terminal blending, or both.

These figures agree in a general way with those obtained
by Jacchia (1954) for a group of 137 bright Super-Schmidt
meteors. He found wake in 46 percent of the cases, terminal
blending in 34 percent, both in 16 percent, and either in
61 percent. The higher percentages are the result of his
greater average meteor brightness. Jacchia notes that all
meteors of maximum apparent brightness of more than four
magnitudes above plate limit show some wake. The indication
is that all meteors release some wake particles and when the

meteor is large enough, the total intensity of all the particles will be great enough to register on the emulsions. A velocity dependence was also seen in these meteors in the sense that the wake was brighter among the low-velocity meteors than among high-velocity meteors of the same apparent magnitude.

A considerable discrepancy exists between the velocity dependences of terminal blending in the two sets of data. Jacchia found none, but ours is most pronounced. This is probably explained in part by our choice of the terminal blending category for doubtful cases. In addition, a selection factor, to be discussed in Chapter III, in Jacchia's choice of meteors seems to affect his result.

We will, from time to time, introduce more statistical data derived from meteors treated by the approximate techniques.

CHAPTER III

BEGINNING POINTS OF METEORS

A. <u>Meteors Characterized by an Abrupt and Early Rise to
Maximum Light</u>

Certain faint meteors display a light curve that
may best be described as "backwards". In the most extreme
cases the meteor appears at maximum light, rising 1.0 or 1.5
magnitudes above plate limit within the period of time between
the dashes (1/80 sec); it then becomes progressively fainter.
The light curve, measured in magnitudes, on the declining
branch is almost linear in time. The final breaks show
terminal blending. By reversing the time scale, one can
obtain a very plausible representation of the light curve
of a normal high-velocity meteor.

In less extreme cases, these meteors may appear at an
intensity close to the plate limit and show a normal increase
in brightness for several dashes followed by a more or less
abrupt rise to a maximum where the change in brightness
may be abrupt or smooth. As before, terminal blending
is likely to be present in the final dashes.

There are no examples of this form of light curve
among any of the several hundred larger meteors photographed
on small cameras. Abrupt meteors are apparently peculiar to
those smaller objects that can be photographed only with

Super-Schmidt cameras.

Of all the meteors photographed in the first year of the Super-Schmidt double-station program (February, 1952 to February, 1953) and reduced by our approximate method, 13 percent of the meteors could be assigned to this category. Although the observational data clearly demonstrate the existence of a class of abrupt meteors, some examples occur that are hard to classify for one of several reasons: (a) the rise is steeper than normal but not abrupt, (b) the increase in light is noticeable but not great, (c) the light curve falls off rapidly at some point after the rise in such a way that the abnormality might be described as simply a prolonged flare, (d) the discontinuity of the light curve occurs so late in the trail that only a small fraction of the meteor departs from normality, or (e) the meteor shows a mixture of the above effects. We have relied entirely on our subjective appraisal of each case in deciding whether a given meteor should be included in the class of abrupt meteors.

The information derived from the approximate reductions indicate that at least three other qualities are shared, statistically, by such meteors. First, as in the case of wake, abrupt meteors are characteristically a low-velocity phenomenon; nearly a third of all meteors of velocities less than 20 km/sec fall into this class (Table 14).

Table 14

Velocity Distribution of Abrupt Meteors

v ($\frac{km}{sec}$)	No. reduced Feb., 1952- Feb., 1953.	No. Abrupt Meteors	% Abrupt Meteors
10-15	85	27	32
15-20	105	31	30
20-30	151	22	15
30-40	185	11	6
40-50	49	3	6
50-60	47	1	2
> 60	140	5	4
Total	762	100	13%

Second, abrupt meteors are, in general, short in duration. Since the meteors in this study represent a rather homogeneous group with respect to their maximum magnitude, we would expect a homogeneity in the durations of any given velocity group unless some distinction in the physical processes exists between different types of meteors. Table 15 lists the median and mean number of dashes observed for (a) all normal meteors; (b) normal meteors with velocities less than 20 km/sec, and (c) all abrupt meteors.

Table 15

Comparison of the Durations of Normal and Abrupt Meteors

		All Normal Meteors	Normal Meteors, $v < 20$ km/sec	All Abrupt Meteors
No. of Meteors		380	89	100
No. of Dashes	Median	19	23	16
	Mean	23.0	28.8	17.7

The mean values are heavily influenced by a few bright meteors, none of which show an abrupt rise. The median values of the low velocity meteors probably should be used as the standard for comparison, since over two-thirds of the abrupt meteors have velocities in this range. However, any comparison of figures in Table 15 shows a significant decrease in the duration of abrupt meteors.

Finally, terminal blending was detected in about two-thirds of the abrupt meteors and was strongly concentrated among the lower velocity objects. Furthermore, if we describe the blending qualitatively in terms of the number of dashes for which terminal wake was recorded, the velocity effect is even more pronounced. (See Table 16).

Table 16

Extent of Terminal Blending Among Abrupt Meteors

as a Function of Velocity

	$v < 20$ km/sec	$v \geq 20$ km/sec
Percent of abrupt meteors with terminal blending	83%	34%
Average number of breaks with terminal blending among abrupt meteors	5.6	1.3

The preceding table and short duration of abrupt
meteors supply, in part, an explanation for the discrepancy
between our results and those obtained by Jacchia in the
case of the velocity dependence of terminally blended
meteors. To measure decelerations, meteors of great length
are preferred. The very short abrupt meteors are not
suitable and they have probably been selectively rejected
for purposes of accurate reduction. However, these meteors
are just those which show a strong velocity dependence in
the terminal blending characteristic.

The various anomalies of these meteors have in the
past, Jacchia (1954), McCrosky (1955), been very logically
explained as the result of a sudden crumbling of the
meteoroid at the point of the abrupt rise. The resulting
increase in the effective surface area causes the increased
luminosity. Differential deceleration of fragments of
different sizes causes the mass of the original meteoroid

to spread along the trail and obscure the shutter breaks. The duration of the meteor will be that of the largest fragments and not that of a single body and consequently the meteor will not endure. The qualitative data of this study have not produced a result at variance with this description of the phenomenon. Moreover, we will be able to make the crumbling-hypothesis still more plausible by a quantitative statistical study.

We may describe these abrupt meteors in terms of a relatively few observational parameters. The degree of crumbling, as measured by the increase of the effective area, is proportional to the luminosity before and after the discontinuity. It can be seen that in a general way the slope of the rising branch of the light curve is related to the rate of crumbling; and the duration and slope of the declining branch is, in some complex fashion, dependent on the distribution of particle sizes after crumbling. The brightness and degree of the terminal blending are also related to this distribution. The height at the point of disruption, the velocity, and the angle of approach into the atmosphere complete the list of the important quantities that may be obtained without recourse to the accurate reduction methods.

Unfortunately, one of the most interesting pieces of information is not available in many of the cases studied. Very often the meteor shows no image before the steep rise

and we can only fix an upper limit on the effective area
of the body before fragmentation. This upper limit is
set by the limiting magnitude of the film, which is itself
a function of the length of the dash (a long and faint
dash can be as easily detected by eye as a shorter but
brighter dash). Since the dash length depends on velocity,
we will introduce an extraneous velocity dependence on the
intensity increase, ΔI, in the sense that the larger values
of ΔI will occur for higher velocity meteors. Even in
those cases where the meteor shows several faint dashes
before the burst, the value of ΔI may be in error by an
amount corresponding to 0.3 or 0.4 magnitudes because of
the difficulty of estimating the brightness of low-intensity
images.

We are in a better position with respect to height.
The common point is extremely well determined because of
the discontinuity in the light curve. The velocities, too,
should be of good quality in so far as they depend on the
ranges. Of course, these meteors are short and the
determination of the radiant distance, r, by the direct
method is somewhat less reliable.

If the assumption of rapid crumbling of the meteor
is valid, we might expect the disruption to occur
because of an internal explosive phenomenon or because of
crushing caused by external pressure forces. We might
also include the possibility that gross fracturing occurs
as a result of a temperature differential through the

meteoroid. We believe that the abrupt meteors supply us
with good evidence that the crumbling occurs when the
dynamic pressure, ρv^2, on the body surpasses the crushing
strength of the meteoric material.

Values of the air density, taken from the Rocket
Panel Atmosphere (1952), were found for the bursting
heights of 74 excellent cases of abrupt meteors.
It was assumed that these heights could be related to the
meteor velocity by an equation of the form:

$$\rho v^n = C \tag{62}$$

or

$$\log \rho + n \log v = \log C. \tag{63}$$

A least-squares solution was applied to find the constants.
These values are compared, in Table 17, with the results
of similar least-squares solutions for the densities at
the beginning heights of normal meteors. We have also
quoted the correlation coefficients, R, for the best
values of $n = n_o$ and for other values of n. The relatively
low probable error for the solution comprising the 74
abrupt meteors is probably indicative of the increased
accuracy resulting from reductions of meteors with well
determined common points.

Table 17

Least-Squares Solution of Equation (63) for Beginning

Points of Normal Meteor and for Bursting Points of

Abrupt Meteors

	Abrupt meteors	All normal meteors	Normal meteors, $v < 40$ km/sec
No. of meteors	74	238	142
$\log C$ (cgs)	4.10	9.42	
n_0	1.94 ± 0.11	2.82 ± 0.07	3.11 ± 0.14
R	$0.84 \pm .03$	$0.91 \pm .01$	
n	1.0	2.0	
R	$0.74 \pm .05$	$0.87 \pm .02$	
n	3.0	4.0	
R	$0.71 \pm .06$	$0.83 \pm .02$	

The normal meteors used for comparison were the first
group of meteors to be reduced. Additional data are
available at this time but have not yet been utilized in
a least-squares solution. Such work will not be carried
out until after the approximate reduction program has been
completed, and after a study of errors has been made by
the comparison of a larger number of cases treated by both
the accurate and the approximate systems of reduction.

However, the probable errors leave no doubt that the
beginning points of these faint normal meteors occur according
to a law different from that obeyed by the bursting points
of abrupt meteors.

By selecting only the excellent cases of meteors
with abrupt rise, we gain the double advantage of using the
meteors with the most accurately known heights, and of
limiting our material to a group of meteors that
indisputably belong to the same class. In this process
we are neglecting about 25 percent of our data and are
also reducing the range of velocities and heights since,
as we have mentioned, the best examples of abrupt meteors
are low-velocity objects. This latter fact suggests
that possibly the $\rho v^2 = $ constant law approached by abrupt
meteors is a result solely of their velocity. However,
a study of low velocity normal meteors (see Table 17) shows
that only a small change in the velocity exponent occurs
for these meteors as compared to that for normal meteors
of all velocities.

Figure 6 shows the relationships determined for the
beginning heights of normal meteors and the bursting
heights of abrupt meteors as functions of velocity. The
filled circles represent individual cases of the beginning
points of normal meteors and the open circles represent
the bursting points of abrupt meteors. In spite of the wide

Figure 6

ATMOSPHERIC DENSITIES AT BEGINNING AND BURSTING POINTS
VERSUS METEOR VELOCITIES
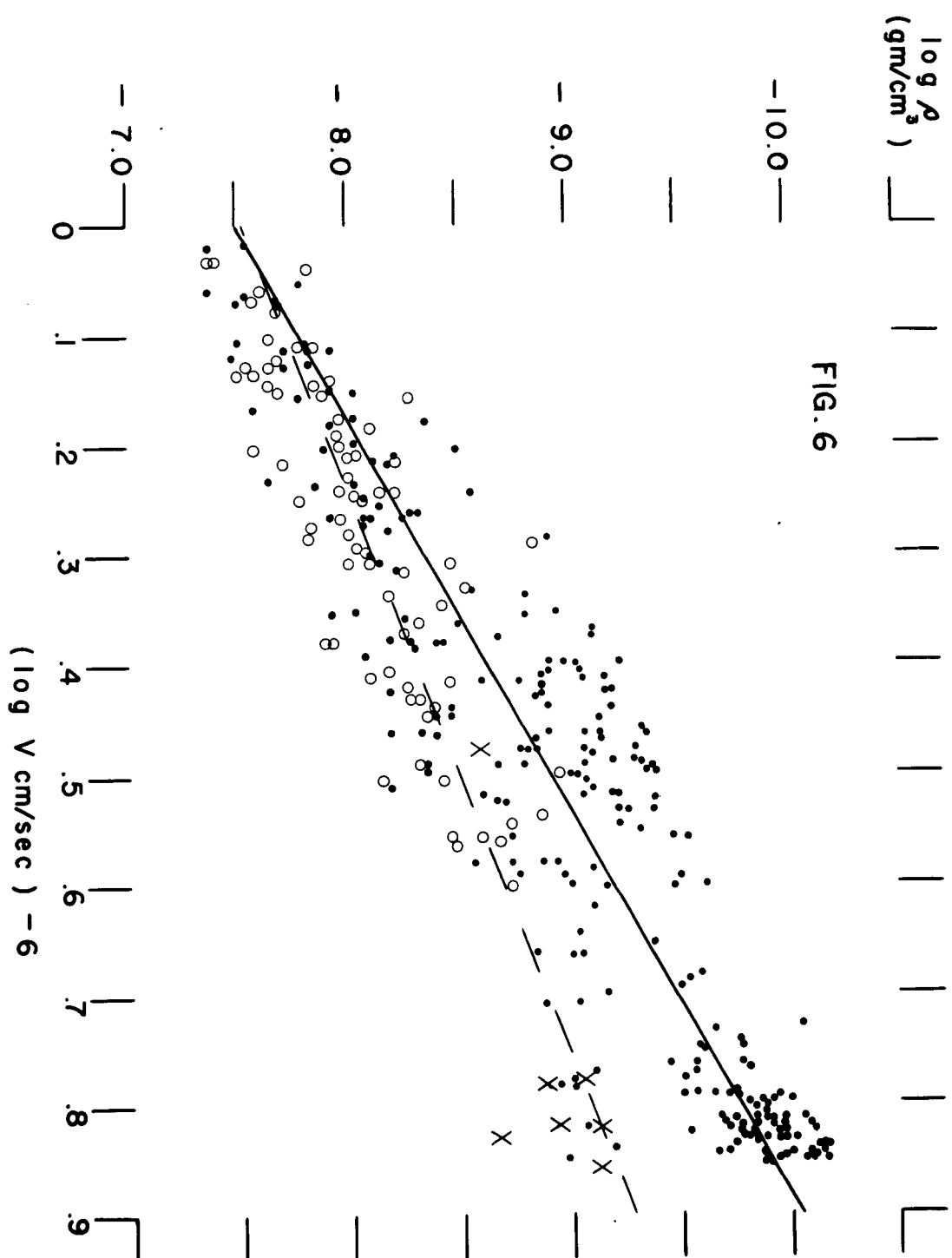
Beginning points of
normal meteors and
least-squares solution
for $\rho v'' = $ constant.

Bursting points of
abrupt meteors and
least-squares solution
for $\rho v'' = $ constant.

Point of disruption
of 7 meteors showing
a hump in the light
curve (data from
Jacchia).

FIG. 6

log ρ
(gm/cm³)

(log V cm/sec) — 6

scatter, most of which is probably real, one can readily see the distinction between the two groups.

Tracing the course of the average meteor by means of this graph, we see that it first reaches a point in the atmosphere at which it may be expected to become luminous. That is, on the classical meteor theory, heat transfer to the body becomes sufficient to vaporize the material. Then at some later time, which depends on the meteor velocity, the pressure on the body (ρv^2) exceeds the crushing strength of a certain class of meteoroids and the abrupt rise in intensity may occur. The scatter that is possible in these points may cause any given meteor, especially if it be a low-velocity object, to be visible first at the fracturing point. However, for high velocity meteors our results predict that in almost all cases the burst will not occur at the beginning point of the meteor. A confirmation of this, and of the result in general, is supplied by seven meteors studied by Jacchia (1949). These meteors showed an unusual increase in luminosity on the rising branch of the light curve. This behavior is abnormal in contrast to the flaring meteors as described by Miss Hoffleit (1933) and Jacchia. Both found flares to occur later in the meteor's trajectory. Also, unlike a true flare, the luminosity of these seven meteors remained high after the burst and did not retreat to the level predicted by the

theoretical light curve. Jacchia tentatively associated
this phenomenon with the atmospheric E-layer but it seems
certain now that the correlation was due to chance. We have
plotted the disruption points (X's) for these meteors in
Figure 6. Their agreement with the constant pressure curve
is good.

B. Beginning Points of Normal Meteors

Our interest in normal meteors in the preceding
section was induced primarily by our desire to compare
them with the special class of abrupt meteors. However,
the result obtained is worth further study and explanation,
even though only an approximate approach is feasible at
this time.

First, we should point out explicitly that the
beginning point is a function of the instrument as well
as of the meteor. It is the first dash image of sufficient
intensity to be photographed and detected by eye on a
careful inspection of the trail. Often the observer will
be able to detect a questionable image (or images) at a
point before the first well defined dash. The beginning
point of such a meteor may be in error by that amount if
the observer incorrectly decides that the doubtful images
do or do not belong to the meteor trail.

We will ask how our observed distribution of beginning points as a function of velocity agrees with the predictions of the meteor theory.

The intensity at any point, given by equations (6b) and (7a), is

$$I = - \frac{\tau_o}{2} \dot{m} \, v^\mu \tag{64}$$

where

$$\dot{m} = - \frac{\wedge}{2\zeta} A \, \delta_m^{-2/3} \, m^{2/3} \rho v^\nu. \ast \tag{65}$$

We have replaced the exponents, 3, by the general quantities, μ and ν. Our result will consist of one equation involving these two unknowns. We have then, the relationship:

$$I \sim m^{2/3} \rho \, v^{\mu + \nu}. \tag{66}$$

$\ast$ Strictly speaking, we should consider both $\wedge$ and ζ as functions of velocity. In the case of $\wedge$, we can only make a negative statement: there is no reason to believe it remains constant.

For ζ, we could refer to the theoretical reaction rate model proposed by Cook, Eyring and Thomas (1951). Under such a hypothesis, higher velocity meteors may acquire energy at such a rate that the surface would be maintained at a temperature in excess of the vaporization temperature. The energy per gram of mass lost would then exceed that determined by the latent heat.

We shall, however, neglect these changes and base our calculations on the classical meteor theory, utilizing $\frac{\wedge}{\zeta}$ = constant.

From our previous result, we know the relationship between ρ and v for average normal meteors. Supposedly, we can find a similar relation for I and v for these meteors. If, then, we can do the same for the masses, we will be able to check the functional representation given by equation (66). To find accurate meteor masses, we must rely upon accurate photometry of the entire meteor trail and the use of equation (10),

$$m_\infty = \frac{2}{\tau_0} \int_{-\infty}^{\infty} \frac{I \, dt}{v^\mu}. \tag{67}$$

Neglecting any change of velocity, we have:

$$m_\infty v^\mu = \frac{2}{\tau_0} \int I \, dt. \tag{68}$$

Jacchia (unpublished) has devised an approximate method for determining the integrated intensity, which we will reproduce here.

Let I_{max} be the meteor intensity at the point of maximum light and I_{lim} the limiting intensity of the plate. We define

$$\Delta M = M_{lim} - M_{max} = -2.5 \log \frac{I_{lim}}{I_{max}} \tag{69}$$

Also, let T, the duration of the meteor, be defined as the time during which the meteor intensity is above the plate limit.

We will employ a gaussian curve to represent the intensity of the meteor as a function of time:

$$I = I_{max} \, e^{-h^2 t^2}. \tag{70}$$

We have chosen the time scale such that $I = I_{max}$ at $t = 0$. Then $I = I_{lim}$ at $t = \pm \frac{T}{2}$. It follows that:

$$I_{lim} = I_{max} \, e^{-h^2 \frac{T^2}{4}}, \tag{71}$$

and

$$h = \frac{2}{T} \left(\ln \frac{I_{max}}{I_{lim}} \right)^{1/2}. \tag{72}$$

From equation (69) we then find,

$$h = \left(\frac{3.034}{T} \right) \left(\frac{\Delta M}{2.5} \right)^{1/2} = 1.919 \, \frac{(\Delta M)^{1/2}}{T}. \tag{73}$$

We can now integrate the intensity, as:

$$\int_{-\infty}^{\infty} I \, dt = \int_{-\infty}^{\infty} I_{max} \, e^{-h^2 t^2} \, dt = .924 \, \frac{I_{max} \, T}{(\Delta M)^{1/2}} = \frac{\tau_0}{2} \, n_\infty \, v^4. \tag{74}$$

The use of the gaussian may be questioned. For low-velocity meteors, the representation may be very good. For high-velocity meteors, whose light curves are not symmetrical, it can be very bad. However, the integrals under the gaussian, as defined, and under the actual curve do not differ greatly. In this case, the proof of this pudding lies in the result of comparing the accurately integrated

intensities and the approximately integrated intensities.
Jacchia finds the agreement to be extremely good ($\sim$5 percent)
in those examples for which a comparison was made.

As a result of equation (74), we may compute the
quantity, $m_{\infty} v^{\alpha}$. The duration is given in terms of the
total number of breaks visible, N. M_{max} (or I_{max}) is
obtained from photometry (see Jacchia, 1949). To determine
M_{lim}, we assume that the magnitude of the meteor at the
beginning point is that of the plate limit, where the plate
limit is defined as the magnitude of the faintest star
visible on the photometric comparison plate possessing
star trails of the same length as the meteor dash.
G. S. Hawkins (unpublished) has kindly supplied us with
his estimates of these values, given as a function of the
length of the star images. The estimates are considered
accurate to within 0.2 magnitudes.

Although we lack precise photometry on meteors treated
in this work, we do have a group among those used in
the beginning point determination for which consistent,
if not absolute, estimates of maximum magnitude have been
made. Using equation (74) we have determined the integrated
intensity of 111 such meteors. The average values of the
logarithm of this quantity, as a function of velocity class
appears in Table 18.

Table 18

Average Integrated Intensity of 111 Meteors

as a Function of Velocity

Velocity class (km/sec)	10-20	20-30	30-40	40-50	50-60	>60	all
Number of meteors	28	28	17	12	9	19	111
log $\int I\, dt$ in arbitrary units	.83	.90	.83	.96	1.19	.80	.87

The scatter in the individual value of log $\int I\, dt$ is considerable but there is apparently very little velocity correlation. A least-squares solution for the exponent in the equation

$$v^n \int I\, dt = \text{constant} \qquad (75)$$

yielded

$$n = -0.1 \pm 0.1.$$

We have, then,

$$m_\infty v^\mu \approx \int I\, dt \approx v^{0.1 \pm 0.1} \qquad (76)$$

or

$$m_\infty \approx v^{(-\mu + 0.1) \pm 0.1}. \qquad (77)$$

Since a negligible amount of material has been lost by the meteor by the time it first becomes visible, we may assume $m_\infty = m_0$.

For information relating to the intensity at the beginning point, we shall consider a group of "average" (to be defined) meteors. We shall assume, as we did in determining the integrated intensity, that the magnitude of the first visible dash is equal to the limiting magnitude of a comparable trailed comparison plate. To convert this to absolute intensity we must make several assumptions, listed below. The numerical values derived from these assumptions will define the average meteor. We assume:

(a) The average distance of the meteor from the radiant, in terms of sin r, is the same for meteors of all velocities. From the average of 100 meteors we determined an average value of $\overline{\sin r} = 0.58$.

(b) The average zenith distance of the beginning point of the meteor, in terms of cos Z, is the same for meteors of all velocities. For the same meteors used in (a), we found this average to be $\overline{\cos Z} = 0.94$.

Table 19 lists the various steps in the correction of the beginning magnitudes (apparent) to units of absolute intensity. The computations are made for 7 average, and hypothetical, meteors with velocities between 10 and 65 km/sec. Rows 2, 3, and 4 give respectively, the density (ρ) at the beginning point, computed from equation (63) and Table 17; the corresponding height above sea level (H) as taken from the Rocket Panel Atmosphere, and the height above the point

of observation (h). Using the average value of cos Z,
we obtain the range, R, from equation (39):

$$R = \frac{h}{\cos Z} = \frac{h}{.94}.$$ (78)

From equation (44), we may now determine the length of
the meteor dash for each of these velocities, by using
the value, $\overline{\sin r} = 0.58$ found above. We may write,

$$v = \frac{\omega' R}{\sin r}$$

or

$$\frac{\omega'}{4} = \text{dash length} = \frac{v \sin r}{4 R}.$$

Row 6 contains the limiting apparent photographic magnitudes
for dashes of this length, as interpolated from Hawkins' values.
In row 7, M_p', we have corrected the preceding value for
the difference of the trailing velocities of comparison
star and meteor, and row 8 is the absolute photographic
magnitude; that is, the magnitude the beginning point would
display had it been at 100 km distance.

The plot of log I against log v (see Figure 7) gives
a graphical solution to the velocity dependence of the
intensity at the beginning point of the normal meteors.
We find that

$$I \approx v^{.69 \pm (?)}.$$ (79)

FIGURE 7 PHOTOGRAPHIC INTENSITY OF
BEGINNING POINTS OF AVERAGE METEORS
AS A FUNCTION OF VELOCITY
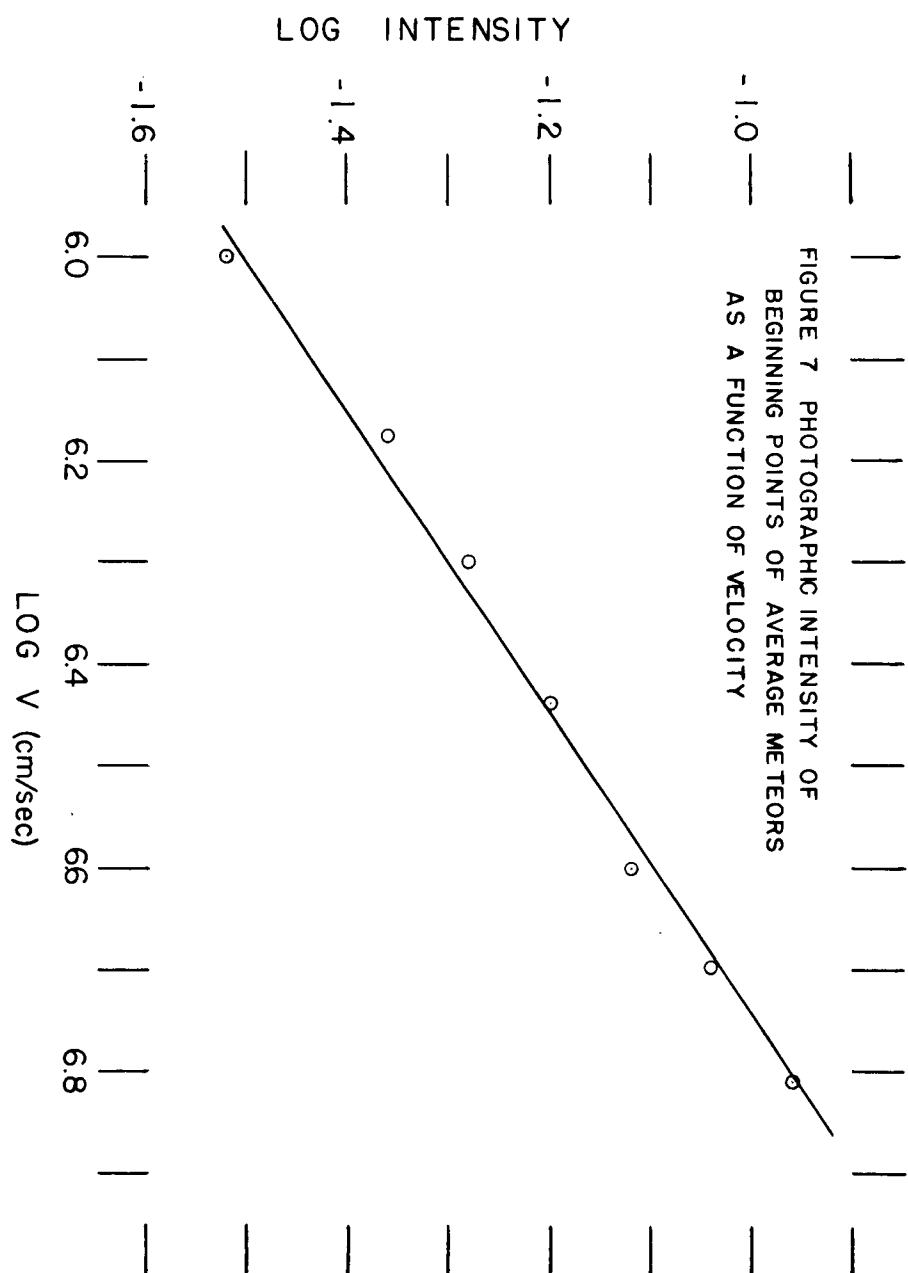
Table 19

Derivation of Photographic Intensities of Beginning
Points of Faint Meteors

Velocity	10	15	20	30	40	50	65
$\log \rho$	-7.50	-8.00	-8.35	-8.85	-9.20	-9.47	-9.79
H	77.5	84.5	89.5	96.5	102.0	106.5	112.0
h	76.0	83.0	88.0	95.0	100.5	105.0	110.5
R	80.8	88.3	93.6	101.1	106.9	111.7	117.5
m_p	10.75	11.00	11.20	11.50	11.65	11.75	11.85
M_p'	3.3	3.1	3.1	3.0	2.9	2.8	2.7
M_p	3.8	3.4	3.2	3.0	2.8	2.6	2.4
$\log I$	-1.52	-1.36	-1.28	-1.20	-1.12	-1.04	-0.96

It is difficult to assess the accuracy of the result
because we cannot be certain of the value of assumptions
(a) and (b).

Summarizing some of our immediate results for the
normal meteors studied here, we have

$$\rho \approx v^{-2.8}$$
$$m \approx v^{0.1} \approx \mu$$
$$\text{and} \quad I \approx v^{0.7}.$$

We expect:

$$I \approx m^{2/3} \rho v^{\mu + \nu} \tag{80}$$

or

$$v^{0.7} \approx v^{2/3} (0.1 - \mu) \, v^{-2.8} \, v^{\mu+\nu}. \tag{81}$$

Equating exponents, we arrive at:

$$\frac{1}{3}\mu + \nu = 3.4. \tag{82}$$

If we assume the values of the standard meteor theory, $\mu = \nu = 3$, a discrepancy of about one half of a power of v exists between our results and those predicted. On the other hand, Öpik's original statement that $\mathcal{T} = \mathcal{T}_o \, v$, which leads to $\mu = 3$, was intended to apply only to bright meteors. He predicted that for smaller bodies, $\mathcal{T}$ would be independent of velocity. And indeed, Jacchia finds that for Super-Schmidt meteors, some improvement in the computed atmospheric densities results when this assumption of constant $\mathcal{T}$ is employed. Our result would tend to confirm this. We have,

$$\text{if } \mu = 3, \qquad \nu = 2.4$$

and

$$\text{if } \mu = 2, \qquad \nu = 2.7,$$

a value which is more compatible with the assumed value of $\nu = 3$.

On the other hand, we might also explain the deviation of equation (82) from the predicted value by a change in ν. The argument in favor of this will be presented in the next chapter.

There can be some question concerning the significance of this general result. The assumptions used are reasonable and the power-law approximations are fair. However, until a more rigorous solution is performed, with a larger number of meteors, this should be accepted as a preliminary result. We believe, though, that the preceding analysis has shown the desirability of repeating the work on a more extensive scale.

CHAPTER IV

THE METEOR WAKE

A. Some Distinguishing Characteristics of Wakes and Trains

The most striking characteristic of the first Super-
Schmidt meteor photographs was the frequent presence of
a considerable amount of luminosity in the shutter
breaks of the trails. The frontispiece shows an example
of this so-called wake. Some such effect had been seen
on a few photographs obtained earlier with smaller
cameras (Millman and Hoffleit, 1937) but in general these
cameras were too slow and the breaks too short for this
phenomenon to be easily apparent. In addition, the shutters
of these earlier cameras were placed in front of the
objective and did not give as sharp a cut-off in the breaks
as do the focal plane shutters of the Schmidts. Thus
it is more difficult to recognize extraneous luminosity
in these somewhat blurred breaks.

We have, in our definition and in our thinking,
distinguished between the phenomena of wake and train. We
have postulated that luminosity in the wake results from
small particles, detached from the meteoroid proper, which
decelerate with respect to the meteor and show a luminosity
behind the meteor. These particles will still have a
velocity comparable to that of the meteor. The train is
supposed to result from recombinations of nearly stationary

atmospheric ions and atoms after the meteor has passed.
The hypothesis that two separate phenomena may cause a
luminosity in the breaks requires justification. Any
simple inspection of the trail cannot distinguish between
the two, and there appears to be no way at present by
which we can show, for certain, that the wake is distinct
from the train phenomena. However, the present data give us
several facts which makes such a distinction entirely
plausible.

First, let us assume that the intensity in the breaks
is due to train, and then ask how the observed character-
istics of this intensity compare with the known character-
istics of a train. We know (Liller and Whipple, 1954),
for example, that trains show considerable more light in
the red than do meteors and we would therefore expect
enhancement of the intensity in the break on panchromatic
film. As yet we do not have an example of the same
meteor photographed on different emulsions but this test
should be kept in mind for the future. However, the
complete lack of success of train photography with blue
emulsions and the existence of strong wake on the same
emulsions are in themselves good evidence for the belief
that the two phenomena are separate.

Some information is also available on the decay time of meteor trains. Liller and Whipple assumed an arbitrary luminosity decay of the form $I = I_0/(1 + Kt)^2$ to fit the observations of meteor trains. The values of decay constant, K, depended on height and ranged in value from 0.3 to 3.0 secs^{-1}. Without concerning ourselves with an exact analysis, a visual inspection of any trail shows that the intensity of the wake has decreased by at least a factor of 2 over a distance of a dash length (1/240 sec). This order-of-magnitude calculation yields a K of 100 secs^{-1}, a value quite out of line with those for train decay. Faults can be found, however, with the above comparison. If, for example, the decay constant itself is a function of time, the comparison is not valid. Liller and Whipple derived their result from the luminosity occurring several seconds after the passage of the meteor, and our data relate to a period of time only several hundredths of a second after the meteor. Perhaps there is no reason to expect the decay factor to be constant over this range. Furthermore, the form of the decay equation may not be at all correct.

A comparison of the statistics of trains and wakes offers a more conclusive method of distinguishing between the two. We have noted (Table 13) that the existence of wake is primarily a low-velocity meteor phenomenon. Trains,

on the other hand, are distinctly associated with high-velocity meteors. Visual observers (Olivier, 1925; Norton, 1946) commonly characterize the Leonid, Orionid, Perseid and other high-velocity meteor showers as train-producing. This writer, on the basis of several years of visual observations, concurs.

The average velocity of 50 meteors in the Harvard program for which trains have been successfully photographed is 59 km/sec. Of these meteors, 40 have been reduced by the approximate method, 9 were treated by precise means and one was identified visually as a Perseid meteor for which we have assumed a velocity of 60 km/sec. We wish to thank Mr. Robert F. Hughes for a considerable portion of the approximate reductions and for supplying these data prior to publication.

Table 20 gives the velocity distributions and the corresponding distribution that would be expected if: (a) meteors produced trains independent of their velocity and (b) the distribution of meteor velocities is that given by Column (a) of Table 12 in Chapter II. The disparity is striking, between the numbers expected and those observed and cannot be explained in terms of observational selection. Although the Harvard observers in New Mexico were cognizant of the older observations concerning trains, there was a period when they thought the majority of trains they

observed visually were associated with meteors of low
(apparent) velocity. However, the effort to verify this
visual observation by photography failed.

Table 20

Distribution of Velocities Among Train-Producing Meteors

v (km/sec)	Observed Number	Expected Number (see text)
10-20	0	15.1
20-30	3	11.4
30-40	5	10.5
40-50	2	3.2
50-60	5	2.4
> 60	35	7.4
Total	50	50.0

Our aim has been to justify our distinguishing between
wake and train, and the velocity criterion is sufficient
to do so. But at the same time we may note that it is
not only velocity that governs train occurrences. The
observations of Trowbridge (1907), Liller (1954), and
Whipple (1953) agree as to the fact that the maxima of meteor
trains lie in the vicinity of 85 to 90 kilometers altitude.
This region is more accessible for meteors of moderate speed
($\sim$30 km/sec) than for very fast meteors. Consequently,
if slower meteors do produce trains, we would
anticipate a larger number, if not a preponderance, of such

meteors among the train data.

The final point in favor of the theory that small particles cause the wake phenomena rests on Jacchia's (1955) interpretation of the anomalous behavior of faint meteors. If fragmentation does occur, we must expect a wake. The amount and the character of the wake will depend on the amount of fragmentation, the size of the fragmented particles and the known circumstances of the meteor itself (velocity, height, and trajectory). The remainder of this chapter will present a quantitative treatment of this problem.

B. Theory of the Meteor Wake

We will assume that at some time, $t = 0$, a small particle, of mass m_o, is separated from the meteoroid. We will further assume that the parent body does not shield the fragment from collision with the air molecules and that the same meteor theory may be applied to meteoroid and to wake particle. The problem will be simplified without any appreciable loss of accuracy if we suppose that the meteoroid does not decelerate during the several breaks over which we will study the fragment. We can now derive the equations giving the intensity of the wake as a function of distance behind the meteor.

The drag equation has been given as:

$$\frac{dv}{dt} = -\Gamma A \sigma_m^{-2/3} \rho m^{-1/3} v^2 = -K_1 \rho m^{-1/3} v^2.$$ (83)

Introducing equation (14), relating the mass and velocity we find:

$$\frac{dv}{dt} = -K_1 \rho m_o^{-1/3} e^{\frac{\sigma}{6}(v_o^2 - v^2)} v^2.$$ (84)

Substituting into equation (84) the relationship,

$$dt = \frac{ds}{v},$$ (85)

we find

$$\rho \, ds = -\frac{m_o^{1/3} e^{-\frac{\sigma}{6}(v_o^2 - v^2)}}{K_1 v} \, dv.$$ (86)

By choosing a suitable scale height, β, we may describe the atmospheric density in a region of several kilometers by the exponential law:

$$\rho = P e^{-H/\beta}.$$ (87)

The height of the meteor at any time, H, is given by $H = H_o + (s_o - s) \cos Z_R$ where Z_R is the zenith distance of the apparent radiant. We will choose our boundary conditions that at $t = t_o$, $s = 0$. All subscript zeros refer to conditions at the time the fragment separates from the meteor. Then:

$$e^{\frac{s \cos Z_R}{\beta}} ds = \left(- \frac{m_o^{1/3}}{K_1 \, P \, e^{-H_o/\beta}}\right) \frac{e^{-\frac{\sigma}{6}(v_o^2 - v^2)}}{v} dv. \quad (88)$$

Replacing $P \, e^{-H_o/\beta}$ by ρ_o and integrating from 0 to s and from v_o to v we have:

$$\int_o^s de^{\frac{s \cos Z_R}{\beta}} ds = \int_v^{v_o} \left(\frac{m_o^{1/3}}{K_1 \, \rho_o} \, e^{-\frac{\sigma}{6} v_o^2}\right) \frac{e^{\frac{\sigma}{6} v^2}}{v} dv. \quad (89)$$

In terms of a new auxiliary quantity,

$$u = \frac{\sigma}{6} v^2, \quad (90)$$

the right hand side reduces to the difference of two exponential integrals and we obtain:

$$\left(e^{\frac{s \cos Z_R}{\beta}} -1\right) = \frac{E_1(u_o) - E_1(u)}{\frac{2 \beta K_1 \rho_o \, e^{\frac{\sigma}{6} v_o^2}}{m_o^{1/3} \cos Z_R}}, \quad (91)$$

or

$$s = \frac{\beta}{\cos Z_R} \ln\left(\frac{E_1(u_o) - E_1(u)}{K_2} +1\right), \quad (92)$$

where

$$K_2 = \frac{2 K_1 \beta \rho_o \, e^{\frac{\sigma}{6} v_o^2}}{m_o^{1/3} \cos Z_R}. \quad (93)$$

The W.P.A. Tables (1940) of the exponential integrals with arguments to four places (0.000 - 9.999) were used for solutions of this equation.

Having chosen values for m_o, H_o, v_o and $\cos z_R$, we computed values of s for various values of v. In general, about 20 such computations were made, representing a range in v of $v_o \geq v \geq v_o$ -10 km/sec. The time elapsed since fragmentation is obtained by quadrature from the tabular relationship v versus s_w (or $\frac{1}{v}$ versus s_w) where s_w represents the distance travelled by the wake particle since fragmentation. Using this and the assumption that the meteor itself travels at constant velocity v_o, we find the lag of the wake particle, behind the meteoroid, to be

$$\Delta s = s - s_w = v_o \, t - s_w. \qquad (94)$$

Since this lag is known as a function of v, we may use the intensity equation to find the luminosity due to the wake particle as a function of the lag, Δs; that is, we may determine the intensity arising from a particle at some given distance behind the meteoroid:

$$I \text{ per particle} = \frac{\tau_o \, \Lambda A 6^{-2/3} \, m^{2/3} \rho v^6}{4 \, \zeta}. \qquad (95)$$

Furthermore, since we know the velocity of this particle and, by assumption, the mass of the particle at the time of fragmentation when its velocity was v_o, we may employ equation (14) to determine the mass of the particle

at the time it decelerates to a velocity v. Substituting
this value of m in equation (95), we obtain:

$$I \text{ per particle} = \frac{\tau_0}{q_\zeta} \Lambda A \delta^{-2/3} m_0^{2/3} \rho v^6 e^{-\frac{\alpha}{3}(v_0^2 - v^2)}. \quad (96)$$

Suppose for the moment that the meteor is at rest
and is a source of wake particles that accelerate away from
the meteor. At the time of fragmentation, the wake
particles have the same velocity as the meteor, i.e., zero
velocity in the present frame of reference. Assume that
fragmentations take place at a constant rate $\dot{m}_p = \frac{dm}{dt}\Big)_p$,
and that this process has continued for a length of time
sufficient to allow the first particles to have accelerated
to some given velocity, say 10 km/sec. Then the current
of particles is in a steady state for a distance equal to
the space required for a particle to reach this velocity,
and a continuity condition exists in this region. In
particular, the numerical linear density of particles
is given by the equation,

$$\mu \left(\frac{\text{particles}}{\text{cm}}\right) = \frac{\dot{m}_p}{m_0 v'} \quad (97)$$

where v' is the velocity of the wake particle with respect
to the meteor at rest. Reverting to the usual frame of
reference, we have:

$$\mu = \frac{\dot{m}_p}{(v_0 - v) m_0}. \quad (98)$$

at the time it decelerates to a velocity v. Substituting
this value of m in equation (95), we obtain:

$$I \text{ per particle} = \frac{\tau_0}{q_\zeta^2} \wedge A\delta^{-2/3} m_0^{2/3} \rho v^6 e^{-\frac{\alpha}{3}(v_0^2 - v^2)} . \quad (96)$$

Suppose for the moment that the meteor is at rest
and is a source of wake particles that accelerate away from
the meteor. At the time of fragmentation, the wake
particles have the same velocity as the meteor, i.e., zero
velocity in the present frame of reference. Assume that
fragmentations take place at a constant rate $\dot{m}_p = \frac{dm}{dt}\Big)_p$,
and that this process has continued for a length of time
sufficient to allow the first particles to have accelerated
to some given velocity, say 10 km/sec. Then the current
of particles is in a steady state for a distance equal to
the space required for a particle to reach this velocity,
and a continuity condition exists in this region. In
particular, the numerical linear density of particles
is given by the equation,

$$\mu \left(\frac{\text{particles}}{\text{cm}}\right) = \frac{\dot{m}_p}{m_0 v'} \quad (97)$$

where v' is the velocity of the wake particle with respect
to the meteor at rest. Reverting to the usual frame of
reference, we have:

$$\mu = \frac{\dot{m}_p}{(v_0 - v) m_0} . \quad (98)$$

Multiplying equation (96) by equation (98), we obtain
a quantity, designated by $\mathcal{L}$, which we will call the
linear intensity. This is the energy per second emitted
by a unit length of the stream of wake material. We have
then:

$$\mathcal{L} = \frac{\gamma_0}{2} \frac{K_1}{\sigma} \dot{m}_p \, m_0^{-1/3} \rho v^6 \frac{e^{-\frac{\sigma}{3}(v_0^2 - v^2)}}{(v_0 - v)}, \quad (99)$$

where we have also multiplied numerator and denominator by
Γ in order to transform the constants into the measured
quantities, K_1 and σ.

It will be noted that equations (92) and (94), relating
the lag and velocity, refer to a particle that has been
fragmented at some given height, H_0, and the intensity that
we derive is the intensity of this particular fragment at
each point in its lifetime as it retards with respect to
the meteoroid. It is this intensity which we have integrated
in order to obtain the expected distribution of light
in the wake, whereas actually the wake intensity at any
given time is due to particles that have left the meteoroid
at different times and, therefore, with a different initial
condition on H_0. Our computations will be meaningful only
if the conditions of the problem are such that those
particles contributing light to the portion of the wake
near the dash are released from the meteor at nearly the

same height as those contributing light far from the dash.
If the meteor velocity is low, the particle size small
and the zenith distance of the radiant large, this condition
will be best fulfilled. We will concern ourselves further
with this error at a later time.

For the convenience of the reader, we shall list the
assumptions made up to this point.

(a) There is no appreciable deceleration of the
meteoroid during the lifetime of a fragment.

(b) All fragments are initially the same size
and shape.

(c) The wake particles fragment from the surface
at a constant rate for at least a period of time equal to
the lifetime of one particle.

(d) Each wake particle reacts with the atmosphere
in the same fashion as a non-fragmenting meteor.

The assumption that we know the values of certain
physical constants is implicit in (d). But the fact is,
we do not. Our values of σ, derived from meteors, are
neither constant nor reasonable. Also, the observed
value of the density of the meteoroid, δ_m --- and thus
K_1 --- may not be the same for parent body and fragment.
For example, if the meteor is a hollow matrix of needles
and each needle is a fragment, both the density and shape
factor would differ from fragment to meteoroid. In the
case of σ, we will employ the lowest value observed for

any meteor, 10^{-12} $(\frac{sec}{cm})^2$, and assume that this value
is representative of a meteor which loses all of its
material by evaporations. For K_1, we will use Jacchia's
(1949) assumed value of 0.76 (cgs). Although an error in
our choice of this constant will affect our fragment masses
considerably, the results will remain self-consistent since
the same factor, $K_1 \, m_0^{-1/3}$, appears in both of our final
equations (92 and 99).

C. Observational Problems of the Meteor Wake-- A Study of a Particular Case

One meteor trail has been treated in considerable
detail by the method given above. The procedure and
results of this investigation are of general interest and
will guide us in a following study of the expected
distribution of wake among meteors of different velocity
classed.

The meteor chosen for study is No. 3567, the one
reproduced in enlargement in the frontispiece. It has
been reduced under the direction of Dr. Jacchia who has
kindly made available the results of the measurements
and photometry. Some of this information is outlined
in Table 21.

Table 21

General Information Relating to Meteor No. 3567

Film No.	ST 945
Date	Aug. 15, 1952
$H(n = 1)$*	100 km
$H(n = 28)$*	91 km
$H(n = 38)$*	88 km
V_∞	26.8 km/sec
$v(n = 28)$	26.6 km/sec
$\cos Z_R$	.717
m_∞	.051 grams
$\log \sigma_{obs}$	-10.9
No. of dashes, N	40

*(n refers to the dash number, the first visible dash being designated as number 1).

A low-velocity meteor was chosen to eliminate any effect of train. The analysis is based on the assumption that the entire luminosity in the breaks is due to the small particle ablation.

The curved film of the Super-Schmidt has been copied on a flat glass plate for measurements by Jacchia. The positive was used to make an enlarged (4x) negative of the meteor trail and its environs. This plate was traced along the meteor trail on a Baird densitometer, operated

with a slit width of about 1/50 of a dash length. With this
densitometer, drift in the tracing can be severe if the
intensity of light falling on the photocell is below a
certain level. The use of the enlargement permitted the
use of a relatively narrow slit without forcing the
instrument to operate in this low sensitivity range.
Furthermore, since our interest is primarily in the wake,
the use of a negative rather than a positive print
eliminates any possibility of drift being important in
the breaks. The relatively slow rate of change of density
in the dash makes the drift problem negligible in those
regions. The diffusion resulting from the finite slit-width
has been neglected in the calibration procedure.

The interpretation of such tracings is not a standard
photometric problem. In the tracing of a spectrum, for
example, the length of slit is not an important factor, for
the density profile along the slit is essentially flat.
In the case of the meteor, the profile is nearly bell-shaped
and the densitometer can record only some average density
over the length of the slit. If the shape of the profile
and the shape of the characteristic curve are known, one
can indeed determine the original intensity that produced
the image but the procedure would be time-consuming. And
in any case, we have no first-hand knowledge of the
characteristic curve. Star images can supply this, but we

have preferred to by-pass this step in favor of a more
direct method. The usual method (Jacchia, 1949) of meteor
photometry gives us an intensity scale that applies
directly to the meteor images. We can associate a
densitometer scale reading (which for the reason just
given should not be called a density) with the photometric
magnitude for each dash. For meteor No. 3567 a range
of about 3 magnitudes exists between the extremes in
intensity.

Tracings were made with several different slit
lengths, ranging from a length that slightly exceeded the
breadth of the brightest image to a length of half this
amount. In each case a good linear relationship between
scale reading and observed magnitude was obtained. The
shortest width was finally employed since it gave the
greatest contrast in scale readings.

Since the maxima of intensity of the dashes on this
meteor do not exhibit flat tops, there is some question
concerning what scale reading should be attributed to
the observed magnitude. In comparing meteor dashes with
trailed star images, as is done in visual photometry, one
would expect the eye to judge on the basis of an extended
image and thus derive some integrated magnitude that was
less than that of the maximum. Since photometry is carried
out with star images which are trailed a distance equal to

the length of a meteor dash, we decided to accept the value
of the scale reading at the point where the rising and falling
branches of the scale-reading curve were separated by a
distance of 1/2 dash length. This is roughly comparable
to assuming that the individual responsible for the
photometry chooses for comparison a star image whose
density would be equal to the density of the meteor if the
intensity causing the meteor image had been smoothed out
evenly over one dash length. We have not looked for an
exact criterion here, we can only make an intelligent
approximation. The final results do not depend critically
on our choice in this matter.

Figure 8 gives the results of this calibration. The
magnitudes are absolute photographic. The curve is based
on 40 points representing photometric estimates and
densitometer readings on as many dashes. Jacchia considers
these magnitudes to be accurate to within $0^m.1$ or $0^m.2$ in
regions of moderate density.* The individual points are
compatible with this estimated figure. Depending on
individual preference for results obtained by an
experienced visual observer or for those obtained from an

---

* Jacchia has employed no correction for any reciprocity
law failure that may exist between meteor exposures ($\sim 10^{-3}$
seconds) and trailed star images (~ 1 second). We have
followed this procedure here although we believe the need
for such a correction may well exist. The question must be
considered open until more information on the emulsion
becomes available.

FIGURE 8   CALIBRATION CURVE FOR
METEOR NO. 3567
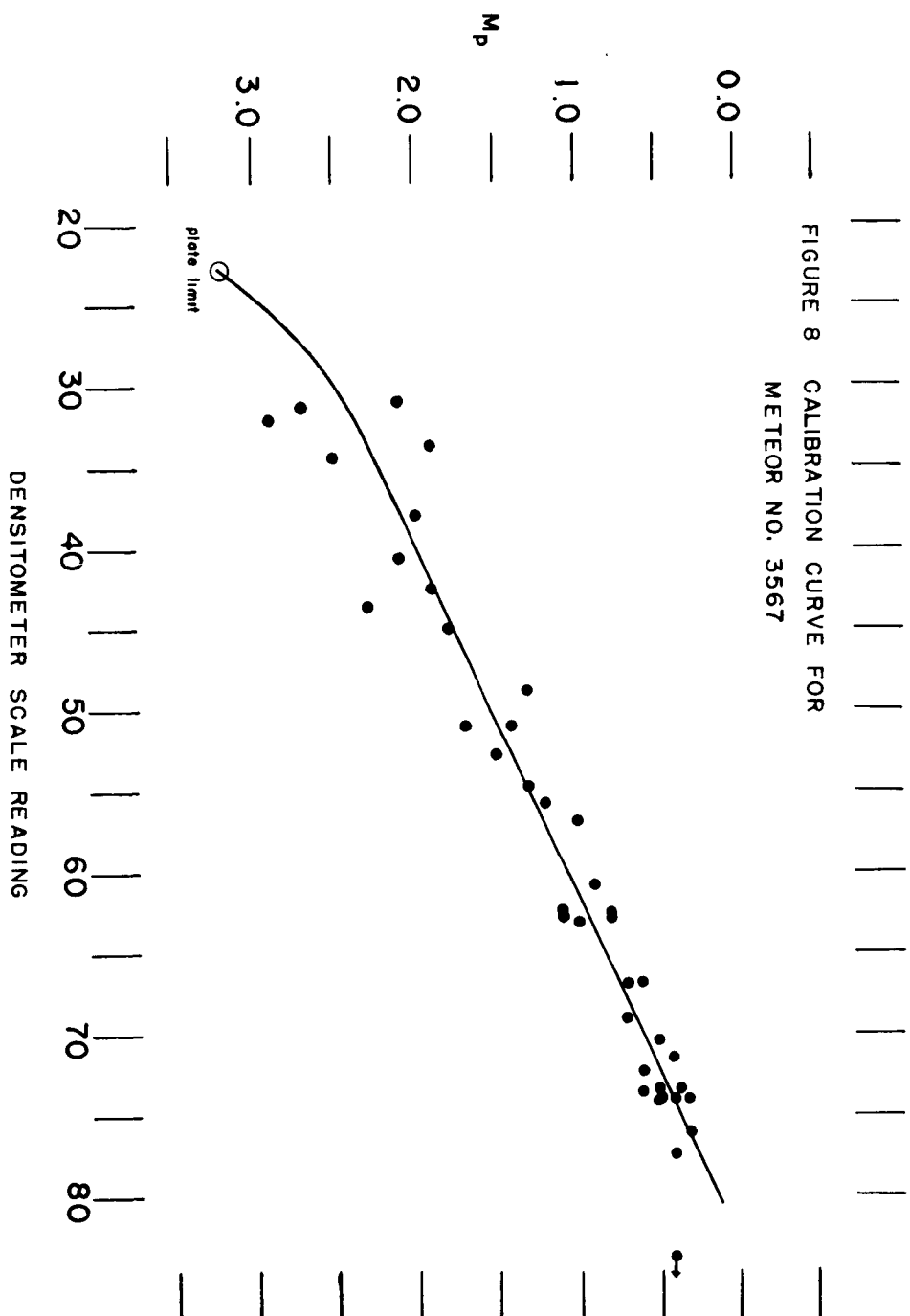
accurate densitometer necessarily used ineptly, one can
justify the accuracy of the other.

For the study of the wake, six dashes (n = 25 to 31) were
chosen. The meteor shows strong wake in this region. These
breaks do not differ markedly from one another and the
tracings indicate that no stars of appreciable brightness
are superimposed on the trail. However, we decided to
average the scale readings, rather than intensities, for
these breaks in order to diminish the importance of any
fainter star images that might be present. Before the
averaging process could be carried out, it was necessary
to determine some zero point in each dash tracing. The
point of maximum light appeared to be the obvious choice
of a well defined position on each break. It was found,
though, that the distances between maxima did not change
monotonically. It was rather surprising to find, then,
that the points of minimum light were separated by a nearly
constant distance and offered a far better choice of a zero
point.

Scale readings were recorded for 26 points, separated
by equal intervals, in each of the six break and dash
cycles. These may be found in Table 22, reproduced here
in place of the actual tracings. The homogeneity among
the six breaks will be noted. The last column is the
average density profile. It is this observed average of the
six shutter cycles that we will attempt to reproduce by
computations. Curve A, Figure 9, shows in graphical form

Table 22

Values of Scale Readings for Selected Positions on

Six Shutter Cycles of Meteor No. 3567

Break No.	26	27	28	29	30	31	(Average)
Fraction							
0	35.0	38.7	37.0	37.2	37.3	35.3	36.75
1	35.2	38.9	38.0	37.6	36.9	35.6	37.03
2	36.8	39.6	39.2	38.7	37.3	36.7	38.05
3	38.1	40.4	40.1	40.6	38.8	38.2	39.37
4	40.0	41.7	41.5	42.8	41.0	40.3	41.22
5	42.0	43.1	43.2	44.9	43.5	42.8	43.25
6	44.2	45.0	45.5	46.9	47.1	45.0	45.62
7	47.0	47.6	48.7	49.9	50.0	48.4	48.60
8	49.8	50.2	51.2	54.3	53.1	50.7	51.55
9	54.0	53.9	55.2	58.2	57.0	53.0	55.22
10	58.6	58.7	59.2	62.9	61.3	56.8	59.58
11	63.3	63.3	64.1	66.4	65.1	61.0	63.87
12	68.0	68.6	68.0	70.7	68.6	65.0	68.15
13	72.3	72.8	71.4	73.3	71.8	70.0	71.93
14	74.8	75.2	74.1	74.9	73.8	73.3	74.35
15	76.0	76.1	75.1	75.3	75.1	76.3	75.65
16	76.1	76.1	75.5	74.8	75.9	78.4	76.13
17	75.3	74.8	75.0	73.7	75.7	78.3	75.47
18	73.0	72.4	73.5	71.8	75.0	76.6	73.72
19	68.8	68.3	69.9	69.0	71.6	73.1	70.12
20	63.0	61.8	64.3	66.3	66.0	68.5	64.98
21	55.0	54.7	59.0	61.0	60.0	61.7	58.57
22	46.9	47.5	53.0	55.4	52.6	53.9	51.55
23	42.3	41.7	46.8	49.3	46.4	45.2	45.28
24	39.4	38.7	41.7	44.5	41.7	39.5	40.92
25	38.6	36.9	39.0	40.3	37.2	36.1	38.02
26	38.6	36.9	37.4	38.0	35.7	35.2	36.97

the densitometer readings as a function of the break-dash cycle ($\Delta n = 1$ represents one shutter cycle). The round top is characteristic of each dash and is not a result of smoothing by the averaging process. It should also be noted that the scale readings for most of the cycle lie between

Figure 9 Observed Density Profile (A) and the Results of Three Attempts to Correct for Diffusion. (See Text)
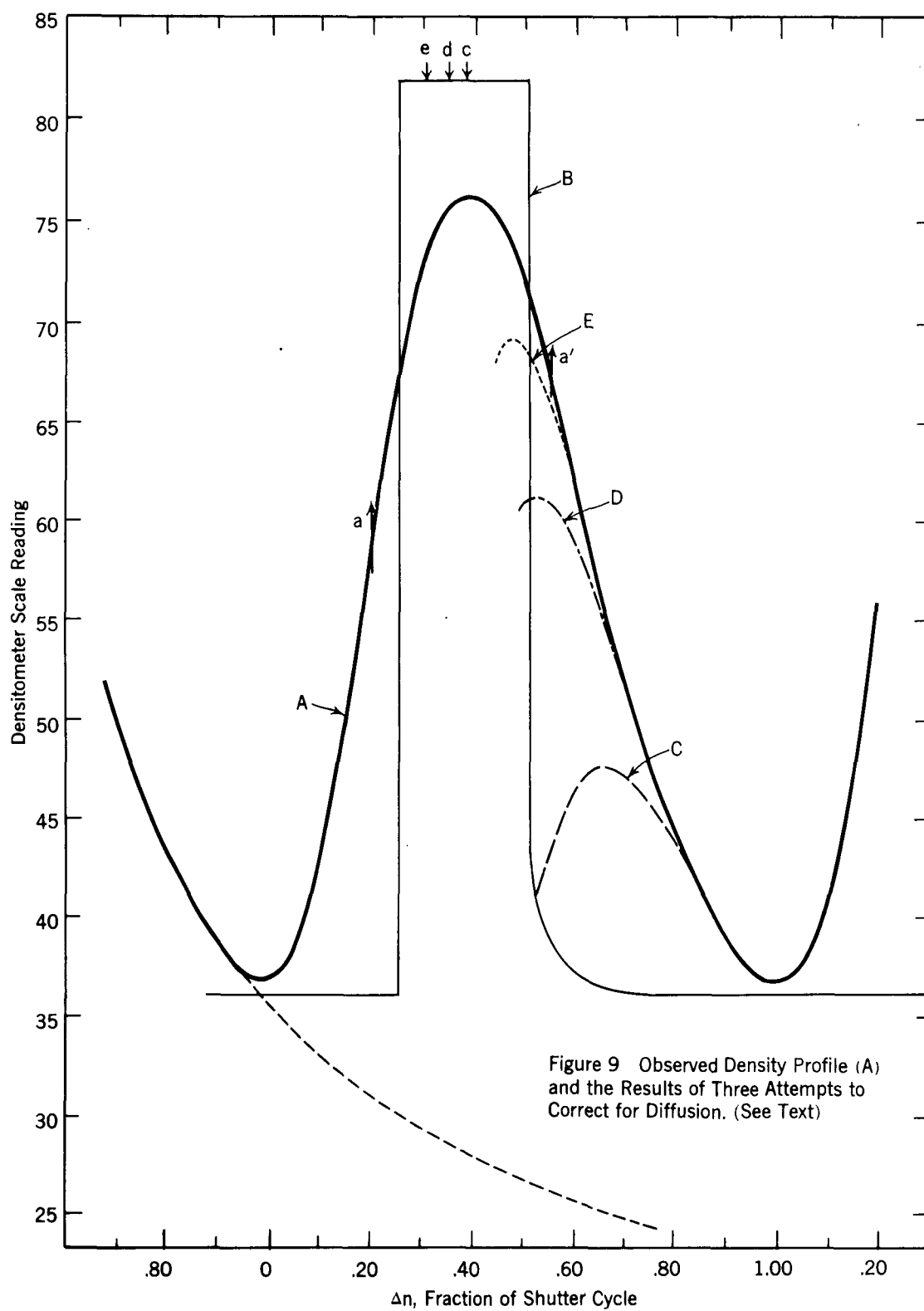
40 and 75 where the calibration is best determined (see
Figure 8). This was not a matter of pure chance. Meteor
No. 3567 was selected from several dozen others for a
variety of reasons. Its low velocity and assumed absence
of train have been mentioned. The appearance of the
strong wake, well above the photographic threshold value,
is another. A stronger wake image could have been obtained
by choosing a meteor in poorer projection against the plane
of the sky, i.e., a meteor at a smaller distance from the
radiant, but this would have intensified the problem of
correcting for the photographic diffusion of the meteor
image into the wake. The present example is a compromise
between high density images and low diffusion.

Our general approach to the analysis of these raw data
originally followed these lines:

(a) Correct, by some means, the intensity
profile for photographic diffusion.

(b) Find that size of particle, fragmented
from the meteor, which would cause the observed slope
in the intensity-lag curve of the wake. We do not intend
to insist on the validity of the assumption that particles
of only one size are responsible for the wake, but our
data are not sufficiently good to determine a meaningful
distribution of particle sizes. Thus, the best approach
seems to be an attempt to find that one size which can best

characterize the observations.

(c) In process (b), we have determined one of
the desired factors, m_o, by fitting observed and computed
slopes of the wake intensity curve. The other unknown,
$\dot{m}_p$, in our basic equation (99) is fixed by the integrated
intensity in the wake.

The question of correcting the observed profile for
effects of diffusion becomes, as will be seen, the crux
of the entire problem of meteor fragmentation. For the
first attempt, we made the assumption that the major part
of the light of a meteor was derived from the meteoroid
itself and that, consequently, the wake represented only a
small perturbation on the total light. If this is so, the
maxima of the dash will represent the position of the
meteor after it has traveled half the distance of the dash.
These assumptions would predict an undiffused profile
similar to that of Curve B, Figure 9. We can use the
difference in intensity between the observed and undiffused
curves at any point, say "a" in Figure 9, to the left of
maximum light to correct the corresponding point,"a", an
equal distance to the right of maximum light. As a modest
refinement of this method, we have corrected the leading
edge of the dash to a point determined by the wake of the
next cycle. The dotted extrapolation of Curve A in Figure 9
represents our estimate of this intensity.

The resulting curve in the wake, rectified by the
procedure described above, is expressed as Curve C in
Figure 9. It should be clear from the description of
the method of wake formation that such an intensity
distribution behind the meteor is an impossibility. At
the time of fragmentation, the particles have their highest
velocity, greatest mass and strongest concentration along the
meteor path. All of these factors act to produce a
constant decrease in wake intensity with increasing
distance from the meteor. Only the air density, ρ, can
act to increase the luminosity and this effect is negligible
for particles of short lifetime. We can, by radically
changing our thinking on the wake process, construct a model
to explain this light curve, but we have not found what we
believe to be a reasonable model. We could, for example,
assume that particles disengage themselves from the meteor,
decelerate with respect to it, and then fragment into still
smaller pieces. One would prefer much stronger evidence
for this complicated technique before accepting it.

We can reduce the extent of the departure of the wake
from a monotonic curve by assuming that the maximum light
does not represent the position of the meteor at the center
of the dash exposure. In this case, then, we are assuming
that an appreciable fraction of the light comes from the wake -
a fraction large enough to shift the center of light to an

earlier portion of the dash. If this is true, we are no longer justified in assuming the same excess of light due to diffusion for points at equal distances to the left and to the right of the chosen center. Or, in other terms, the wake is no longer a small perturbation on the total intensity and we must be concerned with the diffusion of _its_ luminosity. Nevertheless, if we were to find that this effect is small (but not negligible), we might conclude that the simplified diffusion correction used up to the present would supply at least a good first approximation.

To test this, several rectified wake curves were computed on the assumption that the center of the meteor would be found at some point to the right of maximum light. Centers were chosen at the points marked d and e. The resulting rectified wake curves are given as Curves D and E, Figure 9. Only when the maximum intensity of the wake approaches that of the meteor do we find a curve that might represent the intensity of fragmented particles. We must approach the diffusion problem in another way; we cannot think of the wake as producing an amount of light very small compared to that of the meteoroid.

The general diffusion equation,

$$F(x) = \int_{-\infty}^{\infty} f(x-\epsilon)\, g(\epsilon)\, d\epsilon , \qquad (100)$$

relates an observed function, $F(x)$, with an (undiffused) function, $f(x)$ through an error function, $g(\epsilon)$ which in this case will be a measure of the degree of photographic image spreading - as caused by aberrations, turbidity of emulsion and seeing - and of the smoothing effect of the finite width of the densitometer slit. To a first approximation, the intensity curve derived from a tracing of a star image may be used as an error function. Several stars near the meteor trail on film ST 945 were traced with the same slit employed for the meteor. These images show a certain amount of trailing but this does not affect the results if the tracing is made with the slit lying parallel to the long axis of the star image.

Because of the characteristic of the reciprocity law failure for the X-Ray emulsion, we cannot use the same calibration curve for meteors and for stars. The Eastman-Kodak Company has supplied us with the reciprocity failure curves for densities of 0.6 and 1.0. Assuming these points lie on the straight line portion of the H-D curve, we can write

$$D = \gamma\, (\log It - \log i) \qquad (101)$$

and solve for the inertia point and the slope at various
exposure times. The results for the two cases, representing
approximately the exposure times for meteors ($\sim$0.001 sec)
and for tracked stars (3 minutes) are found in Table 23.

Table 23

Effect of Reciprocity Law Failure on the Characteristic Curve of X-Ray Emulsion

Exposure time (secs)	$10^{2.5}$	$10^{0.5}$
Density	log It (MC-sec)	
0.6	-1.36	-1.75
1.0	-1.00	-1.44
γ	1.1	1.3
log i	-1.90	-2.22

To interpret the density readings obtained from the
star tracings, we shall use the ratio of $\frac{\gamma\,\text{star}}{\gamma\,\text{meteor}}$ to correct
our calibration curve, Figure 8. Since we wish to
normalize the star-intensity profile, we need not concern
ourselves with any more nearly absolute intensity units.

The normalized profile of the star, as a function of
distance measured on a scale of 1 = break-dash cycle, is
given in Column 2 of Table 24. This observed curve can be
quite well represented by an error function of the usual
form,

$$g(\epsilon) = \frac{h}{\sqrt{\pi}} \, e^{-h^2 \epsilon^2}, \qquad\qquad (102)$$

if we choose the dispersion parameter to be

$$h = 0.35.$$

This computed function is given in Column 3 of Table 24 for comparison.

Table 24

Observed and Computed Intensity Profiles for

Point Source Images

Distance from Image Center	Observed	Computed (h = 0.35)	Computed (h = 0.175)
0	.198	.198	.098
0.025	.178	.175	.096
0.050	.110	.121	.088
0.075	.059	.066	.076
0.100	.024	.024	.061
0.125	.015	.009	.046
0.150	.007	.002	.033
0.175	.001	.000	.022
0.200	0	0	.014
0.225	0	0	.008
0.250	0	0	.005
0.275	0	0	.002

We have stated that the star image profile is a good first approximation to the error function, in that a point-source profile should properly account for most of the diffusing elements of the image and tracing. It fails,

however, in one respect. Meteor images on the Super-Schmidts
are noticeably out of focus compared to star images, because
of the color differences. It has been found that one can
duplicate the character of meteor images by using trailed
star images that are obtained with the focal length shortened
by about 25 to 100 microns. Using the known angle of the
beam at the focus of this $f/0.65$ system, we can obtain a fair
estimate of the increased dispersion resulting from
improper focus. Although the camera is capable of producing
star images of 15 microns, under field conditions of changing
temperature and inexact focal settings, somewhat larger
images should probably be expected. We have assumed them
to be 20μ. A change of focus of 25μ would then almost
double the image size. Such a line of reasoning has led us
to adopt an error function, for the meteor images, of the
same analytic form as that obtained for the star but with
the diffusion modulus, h, equal to half that of the star.
It is difficult to estimate the error that might be expected
in such an approximation. Using an out-of-focus star image
might seem to be preferable to making the assumption concerning
the form of the error curve. Then, however, we would need
a comparison of the characteristic curves of the enlarged
negatives of both the meteor photograph and the out-of-focus
star photograph. In the absence of any real intensity
standards on the star plate, it would be necessary to assume

that the two photographs had been treated identically in
the many processes between the initial photograph and the
final enlargement. The alternative assumption, as used,
of the form of the error curve does not appear to be any
less satisfactory. The writer feels that any estimate of
$\underline{h}$ for meteors between the values of 0.10 to 0.20 could
be justified. If, instead of h = 0.175, we used twice
this value for the diffusion parameter, we can still find
a particle size that will reproduce the observed intensity
curve. In this case, the particle size is less than an
order of magnitude larger than the mass we shall show to be
most acceptable.

Using h = 0.175, we obtain the error function for the
diffusion of the meteor intensity as given in the fourth
column of Table 24. This error function is the one that will
be used in the solution of equation (100).

Our second attempt to correct for diffusion was also
abortive. We used a method due to Öpik and described in an
unpublished manuscript by Bok and de Jonge (see also
de Jonge, 1954). First we "diffuse" the observed function
curve, obtaining

$$F'(x) = \int f(x-\epsilon) \ g(\epsilon) \ d\epsilon, \qquad (103)$$

and then correct the observed function to obtain the true
function by the equation

$$f(x) = F(x) + \left[F(x) - F'(x)\right]. \qquad (104)$$

This is tantamount to the assumption that successive
applications of the diffusion equation will yield the same
change in the ordinate for any given x. Bok and de Jonge
showed that more refined methods were necessary when the
distribution was skew, as is ours. But more important, such
a method must fail when the diffusion is not reasonably
small. The application of this method to our functions
resulted in some negative intensities for the "true" function.
Other logical inconsistencies, related to the ratio of the
intensity in the wake and in the dash, demonstrated
conclusively that we had overstepped the bounds of
reasonableness in attempting to apply the approximation.

Before continuing with the third attempt at correcting
the diffusion, let us return a moment to our first method.
We were led to that approach not only by its simplicity,
but also by a preconceived notion that all meteors produce
most of their light by atomic ablation directly from the
meteoroid. The first approach has shown that at least a
modest fraction of the light arises from the smaller wake
particles. Our third approach, then, will start from the
assumption that all of the meteor luminosity is produced
by the wake particles. This, as it happens, is a better
first approximation, and will make it easier to produce a

second approximation. The greater flexibility results from the independent determination of the diffusion function. We are no longer requiring that the data from the meteor trail alone supply all of the answers.

Let us outline the method:

(a) We first compute, by means of equation (99), the linear intensity, Q, as a function of the lag, Δs, due to particles of some given initial mass, m_0.

For convenience of explanation, we will express the lag, Δs, in terms of a fraction of the shutter cycle, n, by means of the relation

$$n = 60 \frac{\Delta s}{v_0},\qquad (105)$$

where the figure 60 represents the number of shutter cycles per second.

(b) Our computations in (a) do not lead to a quantity that we may observe directly on a meteor photograph. In essence, (a) yields an intensity distribution as a function of distance behind the meteor; this is what we would photograph if an infinitesimally short exposure were made of the meteor. The actual exposures are not of this nature and we must

account for the "smearing" caused by
the motion of the meteor during the
period of time the shutter is open.
As a particular example, the intensity
we photograph at the point where the
dash and the wake join is due to the
sum of the intensity at this point and
at all parts of the wake behind it that
will, as a result of the meteor's motion,
reach this point in space before the shutter
closes again. Since the shutter remains open
for 1/4 of a cycle ($\Delta n = 0.25$), we must
integrate the linear intensity over this
distance. This, stated analytically, is

$$I_{\Delta n = 0} = \int_{\Delta n = 0}^{\Delta n = 0.25} \mathcal{I} \, ds, \qquad (106)$$

or, for the general case,

$$I_{\Delta n} = \int_{\Delta n}^{\Delta n + 0.25} \mathcal{I} \, ds. \qquad (107)$$

These results are obtained by plotting $\mathcal{I}$ as a
function of Δn and by measuring areas with a
planimeter. It will be noted that the part
of the cycle _in_ the dash ($-0.25 < \Delta n < 0$)
receives part of its contribution from the

wake in the next cycle.

(c) Using the true function obtained in (b) and
the error function derived in Table 24, we
apply the diffusion equation, integrating
by quadrature to obtain a computed function
that may be compared with the observed curve.

(d) Primarily, we are attempting to find a
computed curve whose slope will match that
of the observed curve in the region of the
wake. However, since our first approximation
calls for the entire light to arise from
the wake, the comparison of (c) with the
observed function should be made with the
maxima of the two curves superimposed. A
small relative shift between these curves
could be compensated for by the addition
of some light produced by the meteoroid.

(e) Let us assume that we have found the
proper value of m_o to fit the slope of the
computed curve to the observed curve in
the region of the wake. In order to make
the curves match with respect to their
total intensities, we may adjust $\dot{m}_D$ in
equation (99). And, of course, we will at
the same time be adjusting the magnitude of
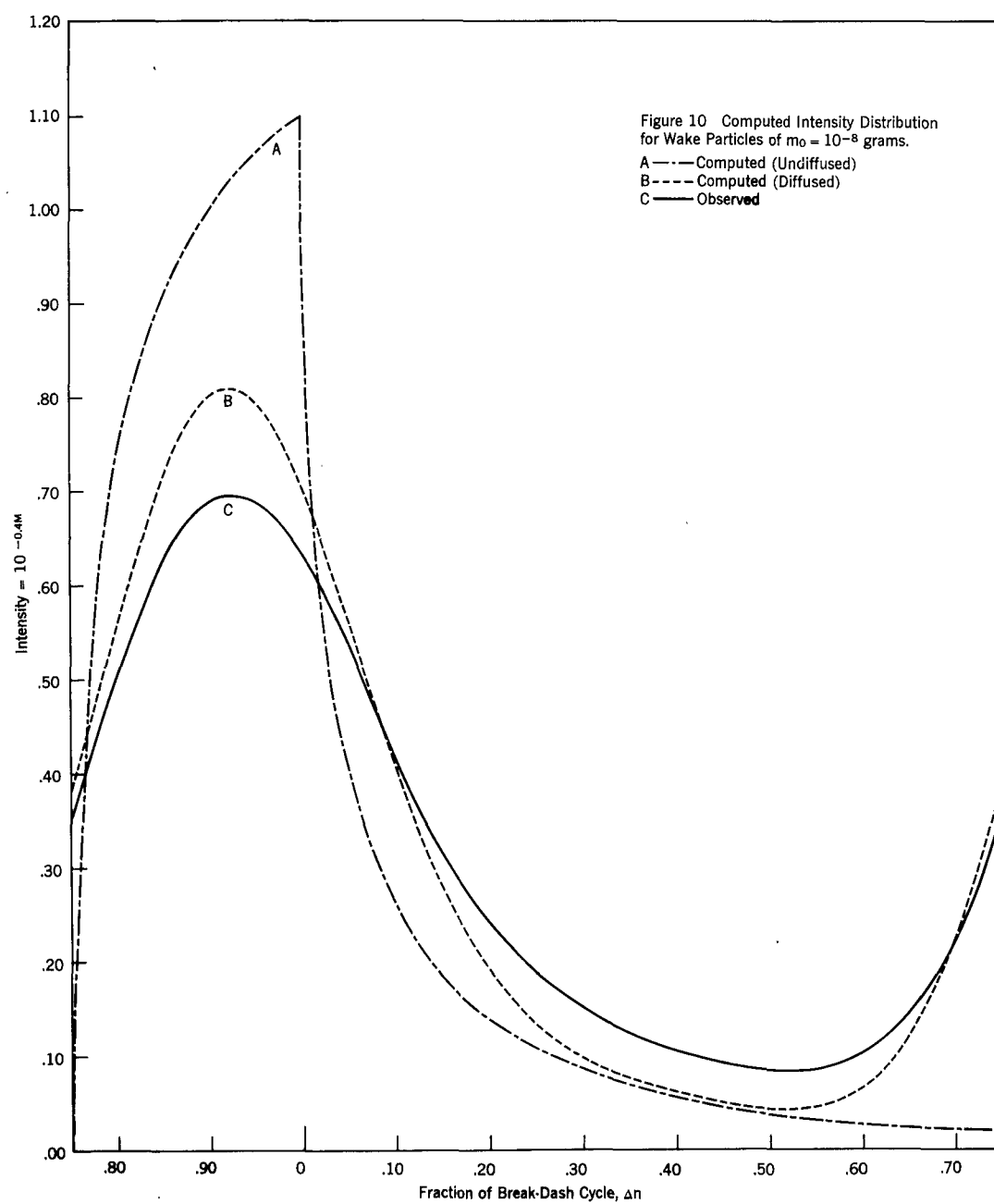the computed curve in the region of the dash.

We require that the computed curve should not
contain a greater integrated intensity than
does the observed curve in the region of the
dash. Allowing the meteoroid to produce
no light is a severe enough change in our
thinking -- we cannot expect it to produce
negative light.

(f) We should expect, if our reasoning and
computations are correct, to find some
value of m_o that satisfies the criteria
of slope and intensity. Such a particle size,
at a given $\dot{m}_p$, will produce the wake and
part, if not all, of the intensity we see in
the dash. Whatever needed intensity the
particles fail to supply to the dash, we will
make up with light from the meteoroid. It
will then be necessary to recompute the
distribution through the diffusion equation,
and to add to the true intensity in the
dash that which is due to the meteoroid. If
this addition is small, one would expect the
second approximation to be sufficient.

This, then, is the procedure we have been forced to
adopt. Mathematically speaking, it is not as nice as the
previous methods. We must perform the computations needed
to "diffuse" the results of light curves for many different
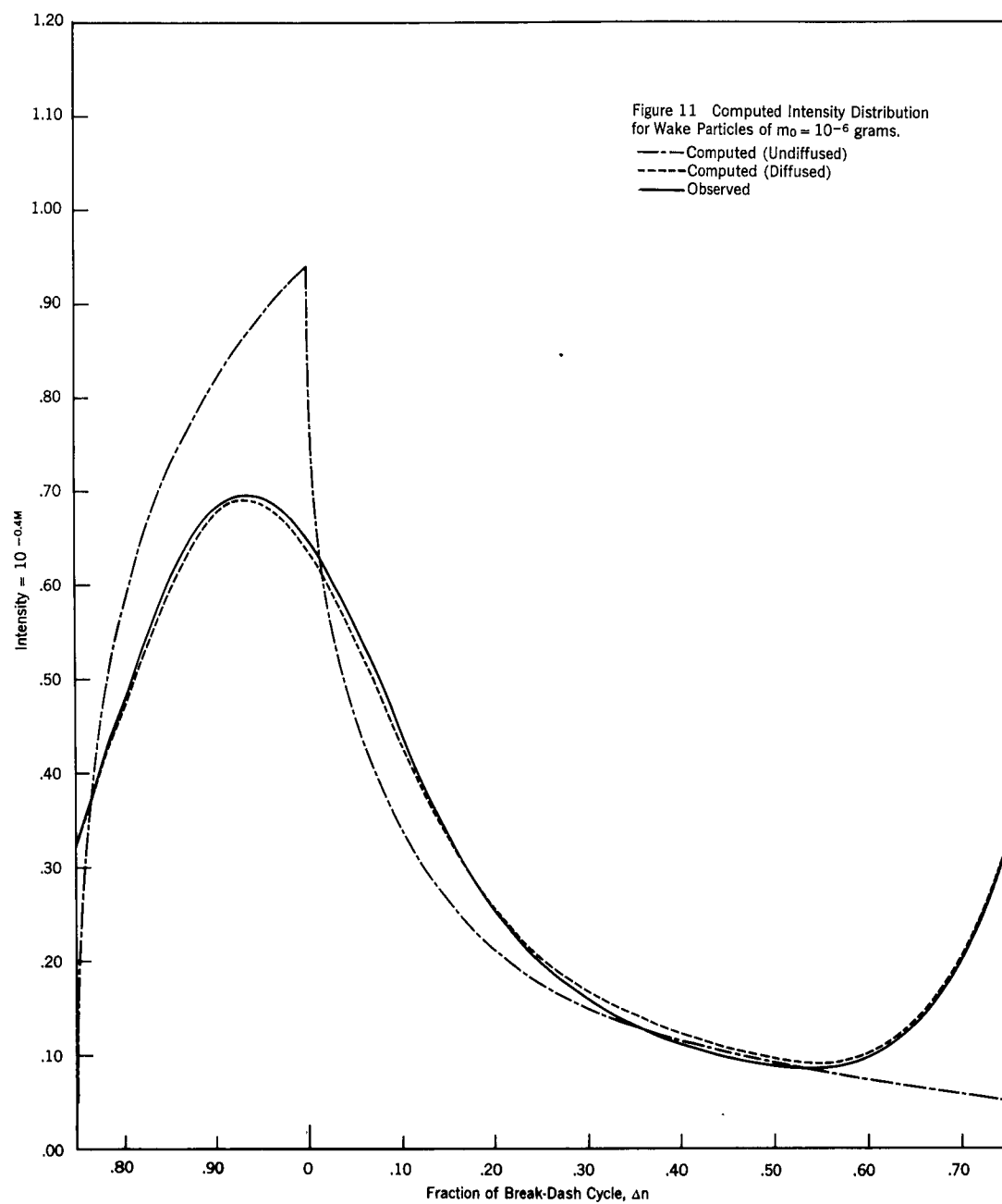particle sizes. In the first trial we used a value of $m_o = 10^{-8}$

grams. Curve "A" of Figure 10 is the computed (undiffused) intensity curve for the wake particles, given as a function of Δn. We have adjusted the amplitude of the curve by assuming a value of $\hat{m}_p$ which equalizes the integrated intensities of this computed curve and of the observed curve, marked "C". Curve "B" is the computed curve diffused by the error function. The computed curve, in the wake, falls below the observed curve. If we force them to match by increasing $\hat{m}_p$, we will increase the total amount of light produced by the particles to a value exceeding the total light observed. Consequently we must adjust the particle size.

There might be some question as to the direction in which we choose to make this adjustment. If we consider the two extreme cases in which: (a), the meteor ablates the smallest particles possible (atoms), and (b), meteor ablates the largest particle possible (meteor breaks into two equal pieces), we see that both cases lead to zero wake-intensity. Between these two extremes, then, there must be some value of m_o which produces a maximum of wake. The familiarity with the equations, gained in the first calculation, is sufficient for us to realize that in the present case we need an increase in the size of the particles.

Figure 10 Computed Intensity Distribution for Wake Particles of $m_0 = 10^{-8}$ grams.
A —·—Computed (Undiffused)
B ----Computed (Diffused)
C ——Observed

Intensity = $10^{-0.4M}$

Fraction of Break-Dash Cycle, Δn

The results for $m_0 = 10^{-6}$ grams, treated in the same
fashion as above, are found in Figure 16. The fit of the
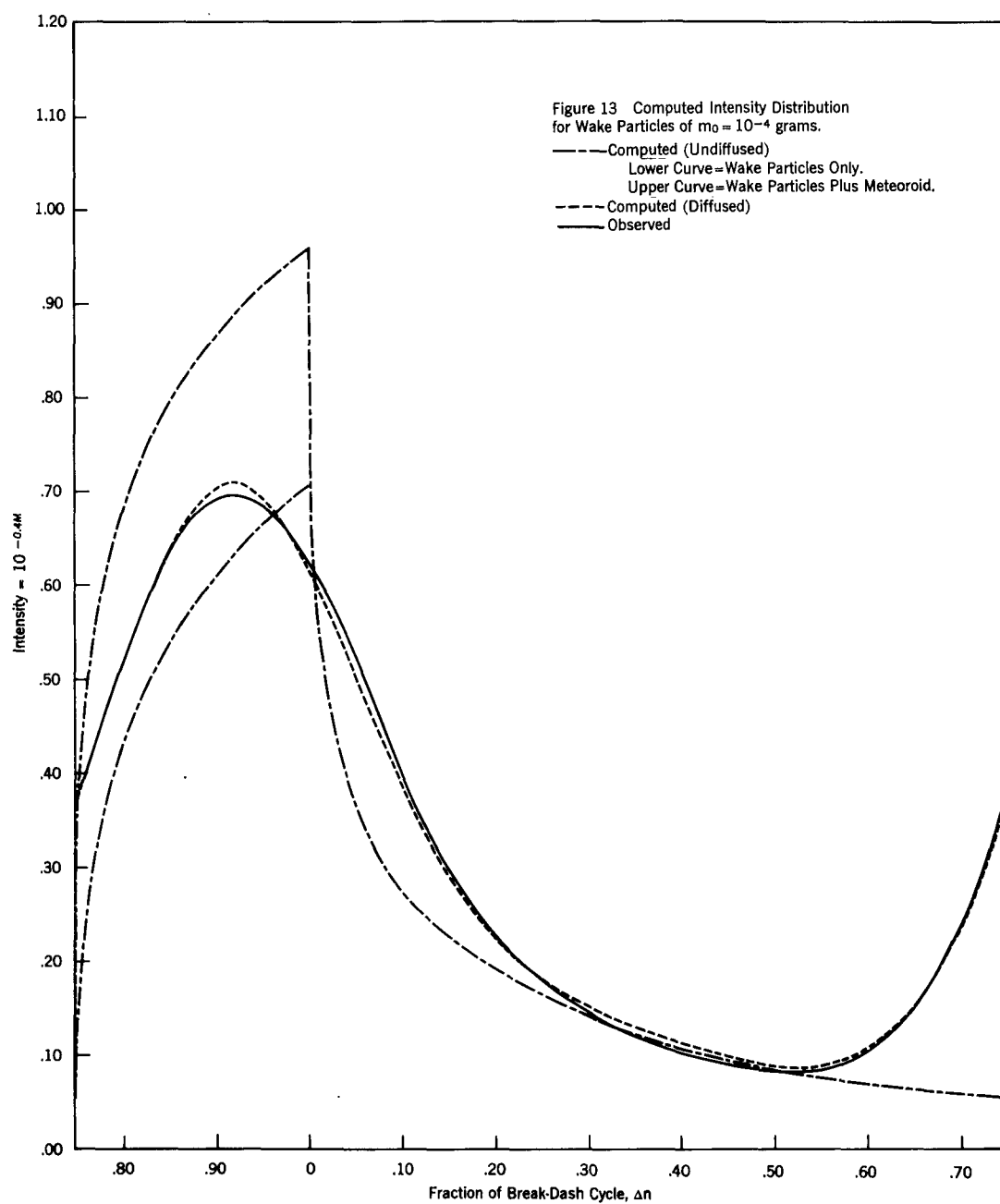observed and computed curves is extremely good. Note that
in this case the entire luminosity can be attributed to
the fragmented particles. Before discussing this result,
we will present, in Figures 12 and 13, the results for
still larger particles, $m_0 = 10^{-5}$ grams and $m_0 = 10^{-4}$ grams.
In both of these cases we can obtain a satisfactory agreement
with the observational curve by a proper choice of $\dot{m}_p$ and
I_b, the intensity produced by the unfragmented meteoroid.
It is probable that agreement could be improved somewhat
for all of the last three cases ($m_0 = 10^{-6}$, 10^{-5}, 10^{-4})
by a more careful selection of the parameters $\dot{m}_p$ and I_b.
The nature and quality of the data make such refinements
meaningless. We may consider that any one of these three
results fit the observations.

The preceding analysis has supplied us with a lower
limit to the particle size that may be used to describe the
meteor wake. Particles smaller than 10^{-6} grams cannot
reproduce the light curve of the wake without exceeding the
total luminosity of the meteor. The upper limit is not as
clearly defined. From the data presented so far, we might
presume that particles of 10^{-3} grams or even 10^{-2} grams could
satisfy all of the observed luminosity conditions. However,
we will show that such particle sizes would not be
consistent with the known duration of the meteor.

Figure 11 Computed Intensity Distribution for Wake Particles of $m_0 = 10^{-6}$ grams.
—·—Computed (Undiffused)
-----Computed (Diffused)
———Observed

Intensity = $10^{-0.4M}$

Fraction of Break-Dash Cycle, Δn

Figure 12 Computed Intensity Distribution for Wake Particles of $m_0 = 10^{-5}$ grams.

—·—Computed (Undiffused)
     Lower Curve = Wake Particles Only.
     Upper Curve = Wake Particles Plus Meteoroid.
— — —Computed (Diffused)
——— Observed

Figure 13   Computed Intensity Distribution for Wake Particles of $m_0 = 10^{-4}$ grams.

— · —Computed (Undiffused)
Lower Curve=Wake Particles Only.
Upper Curve=Wake Particles Plus Meteoroid.

— — —Computed (Diffused)

———Observed

Intensity = $10^{-0.4M}$

Fraction of Break-Dash Cycle, Δn

Depending on the mass of the wake particle, a certain amount of time is necessary for the particle to lag behind the meteoroid sufficiently to produce luminosity in the wake. Figure 14 is a plot of the number of breaks (n) after fragmentation traveled by the meteor before particles of initial size m_0 lag by $\Delta n = 0.25$. The dotted section of the curve is an exponential extrapolation.

Wake becomes obvious in this meteor by the position $n = 14$. If we were to choose a particle size of $m_0 = 10^{-4}$, this would require that an appreciable fragmentation should have taken place before the meteor was visible. Since most of the light of the wake particles is expended at a point in or near the dash, the meteor must be visible as soon as it fragments a sufficient amount to produce wake (unless, of course, the fragmentation occurs at heights so great that the air density is too low for any vaporization to take place). Consequently, we may set an upper limit of about 10^{-4} grams on the particle size that may be used to describe the wake. In this case, the fragments still produce a large amount of the total light produced by the meteor.

Additional information may be utilized to assist us in making a choice of the particle size that should be attributed to the wake. First, we may use the value of σ measured by Jacchia for this meteor (see Table 21) to determine a reasonable ratio of the area of the meteoroid and the total

n (1/60 sec)

25— 20— 15— 10— 5— 0—

FIGURE 14 TIME REQUIRED FOR FRAGMENT
OF MASS m_0 TO ACQUIRE A LAG OF $n = 0.25$
(METEOR NO. 3567)

-9   -8   -7   -6   -5   -4   -3   -2

LOG m_0
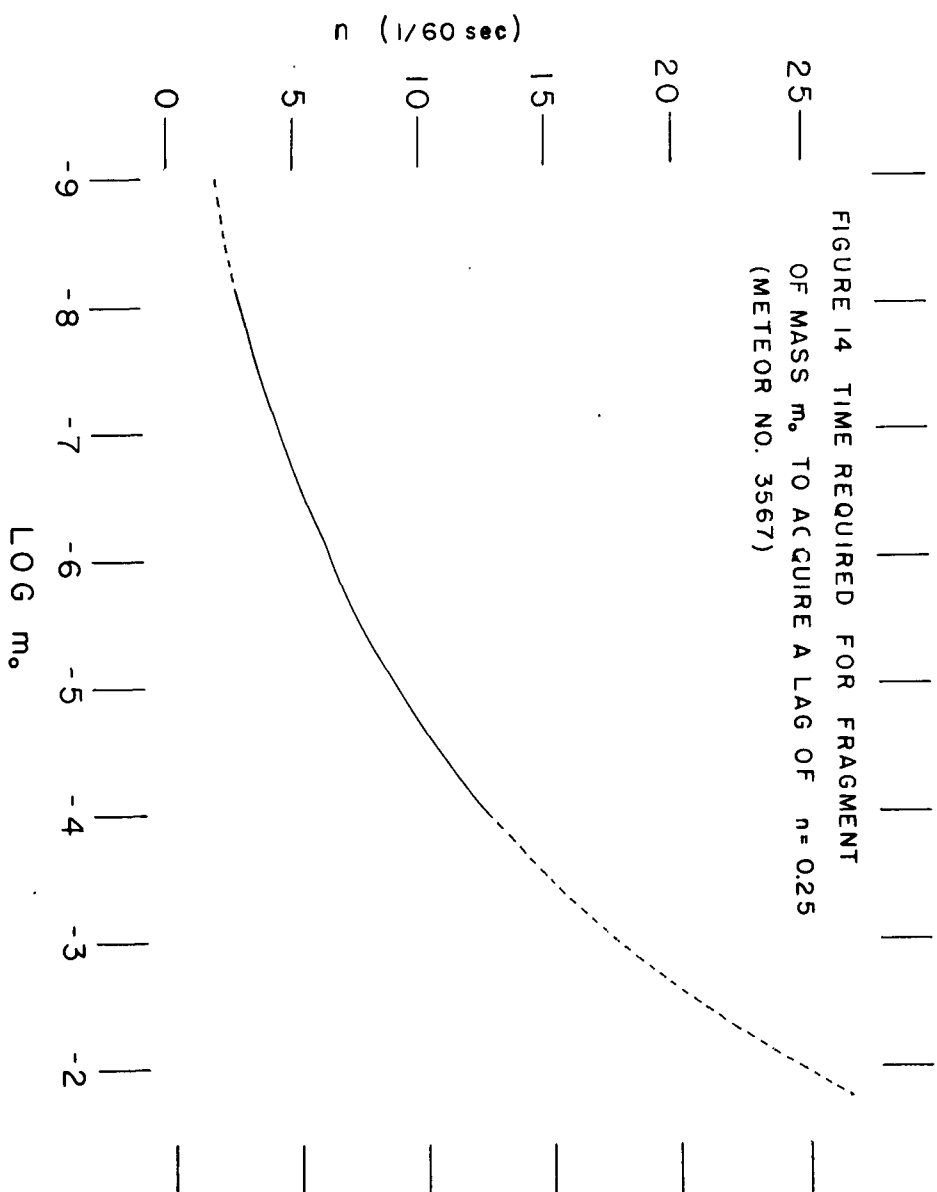
area of the wake particles. We have already derived
(equation (25), Chapter I) this relationship for a meteor
fragmenting in the manner we have assumed for these
calculations. To acquire an estimate of the expected value
of σ_{obs}, we may use the ratio of the luminosity caused
by the wake particles and the meteoroid to represent
the ratio of the areas of the wake particles and
meteoroid,

$$\frac{A_2}{A_b} = \frac{I_2}{I_b} . \tag{108}$$

This would be valid if all the wake particles possessed the
same velocity as the meteoroid; then total intensities would
be proportional to total area. Since the particles produce
most of their luminosity when they are moving at velocities
essentially equal to that of the meteoroid, equation (25)
is a very good approximation.

We will also neglect the correction to σ_{obs} necessitated
by the use of too great a mass in equation (13) (see Chapter
I, page 18). We might estimate that these two effects,
taken into account, would serve to increase the value of
σ_{obs} by less than 25 percent.

Table 25 gives the value of σ_{obs} predicted for each of
the three possible sizes of wake particles. This value is
based on the assumption that the true value of σ is

Table 25

Parameters Derived from Computations Performed to Determine

the Size of Wake-Producing Particles

Initial size of particle, m_0 (grams)	10^{-8}	10^{-6}	10^{-5}	10^{-4}
Rate of mass loss by fragmentation, $\dot{m}_p$ (grams/sec)	.285	.369	.369	.427
Luminosity produced directly by meteoroid, I_b	(<0)	0	.253	.366
Ratio of luminosities of wake particles and meteoroid, I_p/I_b	-----	∞	3.9	2.4
Predicted value of log σ_{obs} (sec/km)^2 (to be compared with -10.9)	-----	∞	-11.3	-11.5

10^{-12} $(\frac{sec}{km})^2$, the value used in the computations. We have

also summarized the other important quantities derived from

the calculations. These results tend to substantiate the

previous conclusions on the best particle size and, indeed,

narrow down the limits of acceptability. The particle size

best suited for reproducing the wake phenomena would appear

to be between 10^{-6} and 10^{-5} grams. It is interesting to note

that this value agrees extremely well with those deduced

by Smith (1954) for meteor flare particles. Since the

ballistic constants employed by Smith agree closely with

ours, we may compare masses directly. His average value,

for 27 determinations of 14 flares, was $5 \cdot 10^{-6}$ grams.

At the time Smith did his work, the concept of very fragile meteors of low density had not been fully developed. The only feasible explanation for flares at that time was one of molten droplets shedding from the meteoroid. If, however, meteors are of such low densities as we now believe, there appears to be no escape from the conclusion that they are a matrix of material. How else shall we form a meteor, which we know contains heavier elements, unless there exists a considerable amount of empty space in the body?

If surface melting occurred in a body of this sort, one would expect the molten material to flow into the interstices. This, coupled with the apparent pressure fracturing of the abrupt meteors (Chapter III) make it seem most likely that all meteoroids fragment solid particles from the surface.

D. The Meteor Wake -- The General Case

We may utilize the information obtained in the previous discussion to inspect some broader aspects of the wake phenomenon. The reader should bear in mind the various inadequacies of the data that yielded the particle size. In particular we wish to emphasize our previous remarks concerning the distribution of fragment sizes. The assumption that one particle size is responsible for the wake phenomenon is almost certainly wrong. On the other hand, the fact that we can fit the observed and computed curves to within the error imposed by our ignorance of the diffusion

function shows that a more complex distribution function
is not justified. Any other hypothetical distribution
that contained an appreciable number of particles smaller
than 10^{-6} grams would also produce a large intensity in
the region of the dash. Our previous qualitative discovery
that the majority of the luminosity is produced by fragments,
would not be altered.

We shall first use our knowledge of the fragment size
to study the effect of the meteor velocity on the presence
of wake. Our observations (page 63) show that wake is more
pronounced, in general, for lower velocity meteors. This
observation is easily understood, in a qualitative fashion,
if the wake is assumed to be composed of small fragments whose
initial size is independent of the velocity of the meteor.
The higher the velocity, the greater the deceleration imposed
upon these particles. Then at any given lag, Δn, the
particles from the faster meteors will have lost relatively
more of their velocity than have the low velocity particles.
As a consequence, their luminosity at this point will be
relatively less and the wake not as pronounced.

This result has been quantitatively verified for
hypothetical meteors at velocities of 15 and 35 km/sec,
as well as for the previous case where $v_0 = 26.6$ km/sec.
For the case, $v_0 = 35$ km/sec, we must make some allowance
for the error caused by the false assumption that all
particles producing the wake at some point are released from
the meteor at essentially the same height. The computations

will show that the meteor will decrease in height by
approximately β (1 scale height) before a particle can
acquire a lag of $\Delta n = 0.5$. We cannot, then, use the same
intensity-versus-lag relationship for the luminosities at
the beginning and at the end of a break. Furthermore,
we may no longer expect that the rate of fragmentation, $\dot{m}_p$,
will remain constant over the time require $(n = 15)$ for the
first fragmented particle to be retarded by $\Delta n = 0.5$. In
order to estimate how this rate will vary, we need not know
the exact process by which particles fragment, but we may
assume that the rate will be proportional to the area of
the meteoroid. Since our calculations have been for the
beginning of a meteor trail, where the area changes slowly,
we may neglect the effect of changing area. Whether the
detachment of the particles results from crushing due to
the dynamic pressure (ρv^2), or to an energy transfer to
the bonds which attach the fragment to the meteor (ρv^3),
we should expect the mass loss to increase proportionally
to the increase in the air density, ρ. The velocity change
of the meteor between $n = 0$ and $n = 15$ will not exceed
several percent and may be neglected. Thus, we may plausibly
estimate that the mass loss would increase in these
circumstances by a factor of e, the ratio of the densities
at heights separated by a scale height. Actually, this
choice of the mass loss may be considered to be dictated by

observation alone. To a good first approximation, the
light curves of most meteors are predicted by the usual
mass-loss and intensity equations, which are based on the
assumption of atomic ablation from the meteoroid. Since the
fragments themselves are ablated in a fairly short time and,
indeed, produce most of their light in a very short time,
the introduction of the intermediate step of fragmentation
will not alter the general shape of the light curve if
the fragmentation does not occur very much more rapidly than
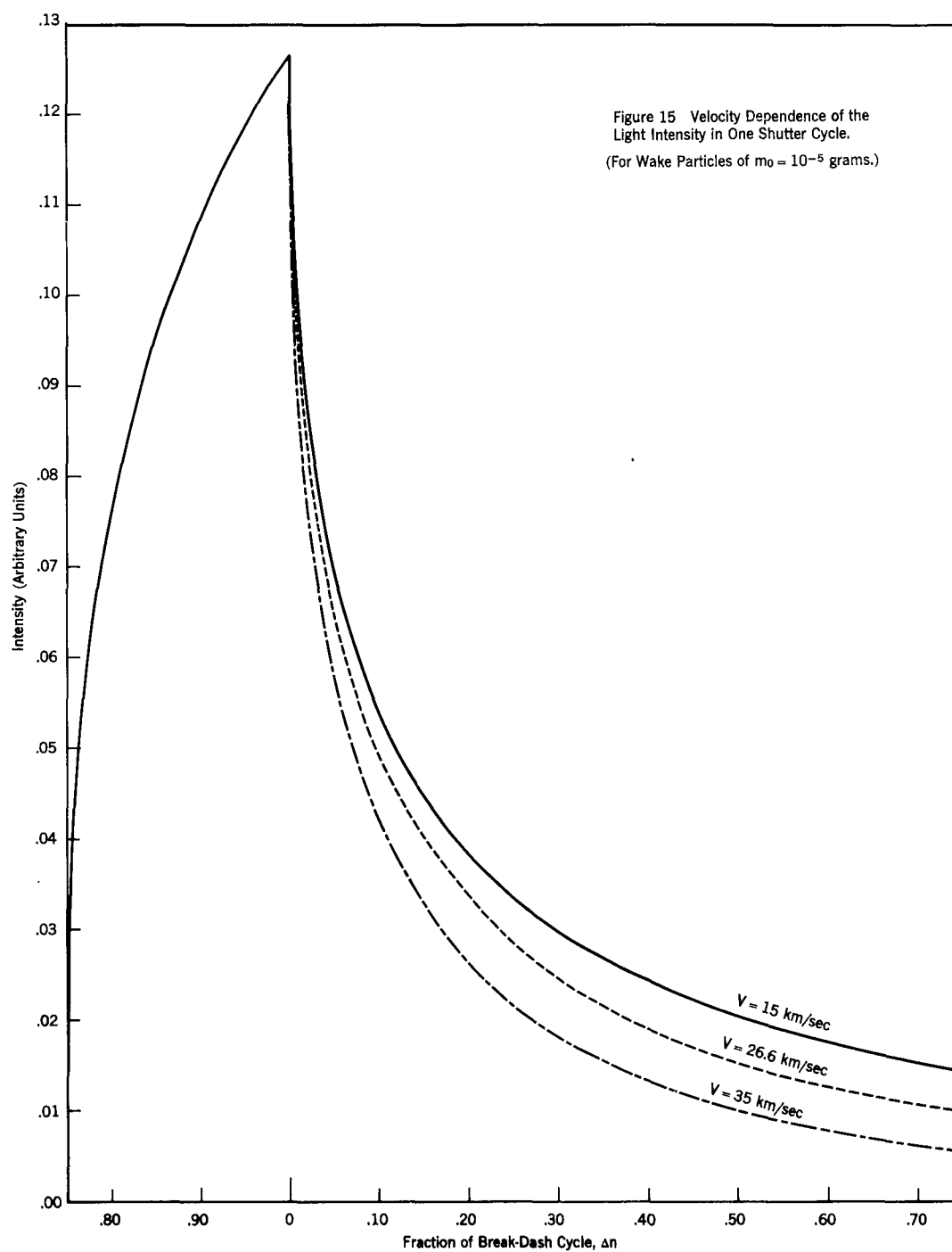the ablation of the fragments.

Consequently, for the case of $v_0 = 35$ km/sec we have
computed the linear intensity versus lag curve (equation
for the two initial conditions of ρ_0 and 2.3 ρ_0 with the
mass losses of $\dot{m}_p$ and 2.3 $\dot{m}_p$, respectively. Intensity
curves were drawn for both of these. We determined the
intensity to be expected for the actual wake by setting
the wake intensity in and near the dash equal to the
intensity derived from particles detached from the meteor
at the dash ($n = 15$), while the wake intensity in the
break ($\Delta n = 0.5$) was set equal to the intensity derived
from particles detached from the meteor at $n = 0$. For
other values of n, a smooth curve was drawn, going in
transition between these two extreme cases. The initial
height, described by ρ_0, is the average beginning height for
faint meteors of this velocity. Cos Z_R has been taken as

0.717, which corresponds to the observed value for the case
at $v_0 = 26.6$, computed previously.

For the case $v_0 = 15$ km/sec, the change in height of
the meteor is small over the time required for the particles
to show an appreciable lag and the extensive corrections
applied above were unnecessary. Also, the initial height
chosen for this computation is the average beginning height
for faint meteors of this velocity. Cos Z_R was taken as the
same value as the one used for the case of $v_0 = 35$ km/sec.

Computations for the case $v_0 = 26.6$, have already
been made in connection with the previous analysis of
meteor No. 3567. These results apply to particles detached
from a meteor at a point 3 km lower than the average
beginning height of meteors of this velocity.

Figure 15 shows the expected intensity in arbitrary
units in the course of one shutter cycle for the three
cases. For comparison we have normalized these curves so
that the total intensity in the dash, $-0.25 \leq \Delta n \leq 0.0$, is
the same for all cases. It is interesting to note that the
differences in velocities here have very little effect in
changing the shape of the intensity curve in the dashes.
Those differences that do exist are of the order of a few
percent, and no attempt has been made to illustrate these
departures from the mean dash curve displayed in Figure 15.

Figure 15   Velocity Dependence of the Light Intensity in One Shutter Cycle.

(For Wake Particles of $m_0 = 10^{-5}$ grams.)

It is clear from this figure that wake should be
expected to be a low-velocity meteor phenomena, as observed.
Three additional factors, not included in the calculations,
modify the preceding results. Our observational data are
entirely visual, and to make a fair comparison we should
take into account the fact that the eye is capable of
detecting a faint and long image as easily as it detects
another image that is brighter but shorter. Since, in
general, the faster meteors produce longer dashes, we should
expect that this effect would partly overcome the ability
of slower meteors to produce a visibly detectable luminosity
in the wake.

On the other hand, we have compared the undiffused
theoretical light curve and our observations are based on
diffuse images. With this correction applied, the shorter
images produced by the slower meteors will have the advantage
that a greater portion of the dash luminosity is diffused
into the break.* This factor will certainly outweigh the

---

*The lesser importance of diffusion on the dashes of high-
velocity meteors can be easily seen on microdensitometer
tracings of such trails. The tracings often show a dash
profile on the same nature as the undiffused curve
plotted in Figure 15. These dashes show a distinct maximum
at the point $\Delta n = 0$, decreasing by as much as 0.5 magnitudes
at the point $\Delta n = 0.75$. This confirms our supposition that
much of the meteor luminosity results from small particles.
Also, it demonstrates the power of the densitometer
technique -- this change in intensity can not be detected by
eye.

visibility argument and will increase the probability that
wake may be detected for low-velocity meteors.

Finally, we have also seen that high-velocity meteors
must persist for a far longer interval of time for wake
to be detected. For example, if our hypothetical meteor
of 35 km/sec velocity had had a lifetime of 10 dashes,
little wake would have been observed, since even those
particles that fragmented at the meteor's beginning would
have been retarded only by an amount $\Delta n = 0.16$. On the
other hand, a meteor of 15 km/sec under the same conditions
would have wake particles at $\Delta n = 0.54$.

On this basis one would expect that the observed
distinction in the velocity of wake-producing meteors would
diminish if one were to observe brighter meteors of longer
duration. Such is indeed the case: essentially all long
meteors display wake, independently of their velocity.
However, this fact may be explained just as easily in terms
of the increased size, and consequent increased mass-loss
and luminosity, of the longer meteors.

E. Terminal Blending

Continuous fragmentation of meteors wherein all or
most of the luminosity arises from small particles offers
a simple and satisfactory explanation of some examples of
terminal blending. This elongation of the final dashes was
reported by Jacchia (1954) to occur in approximately one-third

of the 157 long meteors analyzed. In these cases there
was no good correlation with either velocity or brightness.
Our own results show that this phenomenon does occur more
frequently with low-velocity meteors.

The light curve of a meteor with blended dashes
often shows no abrupt variations from that of a normal
meteor, although the blended section itself is characterized
by a nearly constant intensity, at variance with the ending
of a normal meteor. Blending is most often seen, in faint
meteors, for two or three dashes, but in extreme cases it
has been visible for an estimated 50 dashes. More often
than not, meteors that display a wake are not blended.

Let us consider a normal meteor, with no sharp
discontinuities in the light curve, as it nears the end
of its trajectory. If it has been fragmenting particles,
we may or may not detect a wake, depending on its velocity
and duration. At this point in the meteor's path, the rate
of fragmentation will decrease rapidly due to the decrease in
area and, as a consequence, the luminosity in the region of
the dash will be reduced. However, the luminosity in the
wake may be relatively high, since it results from the
far larger number of particles that were fragmented when
the meteor area was appreciably larger. When the luminosity
due to smaller number of larger masses equals the larger
number of smaller masses, wake and dash will be

indistinguishable and terminal blending will be present.

In those cases where terminal blending occurs suddenly without any previous wake, this approach appears to fail, or at least to require the very special case of wake becoming appreciable just as the meteor ends its trajectory. However, this explanation does overcome the difficulty of a previous suggestion in which it was assumed that the meteor suddenly crumbled near the end of its path, into many pieces of comparable size. Such an overall fragmenting would result in a burst of luminosity, which is not observed.

REFERENCES

Carrol, P. S., McCrosky, R. E., Wells, R. C., and Whipple,
    F. L. 1951 Harvard Reprint II-39, "Film Molding
    and Photographic Accessories for the Super-Schmidt
    Meteor Cameras"

Cook, A. F. and Millman, P. M. 1955 Ap. J. 121, 250,
    "Photometric Analysis of a Spectrum of a Perseid
    Meteor"

Cook, M. A., Eyring, H. and Thomas, R. N. 1951 A. J. 113,
    475, "The Physical Theory of Meteors I. A
    Reaction-Rate Approach to the Rate of Mass Loss
    in Meteors"

de Jonge, J. H. K. 1954 Thesis, Harvard University, "On
    the Absolute Magnitudes of the A-Type Stars"

Hoffleit, D. 1933 Proc. Nat. Ac. Sci. 19, 212, "A Study
    of Meteor Light Curves"

Jacchia, L. G. 1949 Harvard Reprint II-31, "Photographic
    Meteor Phenomena and Theory"

_____ 1954 Status Report No. 7, Meteor Analysis
    Project at Harvard College Observatory

_____ 1955 Ap. J. 121, 521, "The Physical Theory
    of Meteors VIII. Fragmentation as a Cause of
    the Faint Meteor Anomaly"

Liller, W. and Whipple, F. L. 1954 "Rocket Exploration
    of the Upper Atmosphere," (Boyd and Seaton,
    Pergamon Press Ltd., London)

McCrosky, R. E. 1955 A. J. 60, 170 (abstract) "Fragmentation
    of Faint Meteors"

Millman, P. M. and Hoffleit, D. 1937 Har. Ann. 105, 601,
    "A Study of Meteor Photographs Taken Through a
    Rotating Shutter"

Millman, P. M. 1952 J. R. Astr. Soc. Can. 46, 121

_____ 1953 J. R. Astr. Soc. Can. 47, 217

Norton, A. P. 1946 "Norton's Star Atlas," p. 43,
    (Gall and Inglis, London)

REFERENCES (continued)

Olivier, C. P. 1925 "Meteors" (Williams and Wilkins,
        Baltimore)

Öpik, E. 1933 Harvard Reprint 100 "Atomic Collisions and
        Radiation of Meteors"

Rinehart, J. S., Allen, W. A., and White, W. C. 1952
        Jour. Ap. Phys. 23, 132, 198, 297, "Phenomena
        Associated with the Flight of Ultra Speed
        Pellets" (Parts I, II, and III)

Smith, Henry J. 1954 Ap. J. 119, 438, "The Physical
        Theory of Meteors V. The Masses of Meteor
        Flare Fragments"

"Tables of Sine, Cosine and Exponential Integrals" (W.P.A.,
        1940)

The Rocket Panel 1952 Phys. Rev. 88, 1027, "Pressures,
        Densities and Temperatures in the Upper Atmosphere"

Thomas, R. N. and Whipple, F. L. 1951 Ap. J. 114, 448, "The
        Physical Theory of Meteors II. Astroballistic
        Heat Transfer"

Thomas, R. N. 1952 Ap. J. 116, 203, "The Physical Theory
        of Meteors III. Conditions at the Meteor Surface"

Trowbridge, C. C. 1907 Ap. J. 26, 95

Whipple, F. L. 1939 Pop. Ast. 47, 419, "Upper Atmospheric
        Densities and Temperatures from Meteor
        Observations"

_____ 1950 Ap. J. 111, 375, "A Comet Model"

_____ 1951 Pop. Ast. 56, 144, "The Baker Super-
Schmidt Meteor Cameras" (abstract)

_____ 1952 A. J. 57, 28, "On Meteor Masses and
Densities" (abstract)

_____ 1953 Jour. of Meteorology 10, 390, "Winds
in the Upper Atmosphere by Meteor Train
Photography"

_____ 1954 A. J. 59, 201, "Photographic Meteor
Orbits and Their Distribution in Space"

REFERENCES (continued)

Whipple, F. L. and Jacchia, L. G. (in press) Smithsonian
        Astrophysical Contribution, No. 1, "Reduction
        Methods for Photographic Meteors"

Wright, F. W., Jacchia, L. G. and Whipple, F. L. (in press)
        A. J. "Photographic α-Capricornid Meteors"

SUMMARY

The problem of meteor fragmentation is not a new one.
Large meteorites have been observed to burst in flight and
often a meteor fall will consist of a shower of bodies
which are apparently due to the fracturing of a larger body.

However, our concern is not with the massive meteorites,
but rather with small meteors whose maximum intensities
range from $+3^{rd}$ to 0th magnitude. An immense amount of
material has been gathered on such objects within the past
few years through the use of the new Baker Super-Schmidt
meteor cameras.

Two of these instruments, separated by about 18 miles
are used to photograph the same meteor. The cameras are
equipped with rotating shutters that occult the meteor
trail at known intervals. From such photographs, the
intensity, height, velocity and deceleration of the meteor
may be determined. Using the classical meteor theory, one
may either (a) solve for the density of the atmosphere from
the known deceleration or (b) assume the density to be known
and determine those constants, occurring in the equations,
for which we have only estimated values. In recent years,
since the advent of the high altitude research rocket and
the resultant increase in knowledge of the upper atmosphere,
the meteor astronomer has tended to take the second approach.

Investigations by Whipple and by Jacchia have shown
that the average meteor photographed in the Harvard program
must be quite a different object from the meteorite. It
seems entirely likely that the objects are of extremely
low density -- less than that of water. Furthermore,
the characteristics of the light curve of the meteor and
of its dynamic behavior in the atmosphere can only be
explained in terms of a fragmenting body.

Because of the high accuracy of measurement required to
determine decelerations, only a small percentage of the
photographic material has been reduced. We have developed
a rapid graphical method of meteor trail reduction in order
to acquire a greater body of data with which to study
statistical aspects of the faint meteor phenomena.
Reasonable estimates of the mean errors in the computed
heights and velocities are, respectively, 3 percent and 5
percent.

Results for about 1000 meteors are included in this
discussion. In general, these meteors represent a homogeneous
group in terms of apparent maximum magnitude. Consequently,
all meteors of a given velocity group are represented by the
same mass. It is to be expected, on the basis of the
present meteor theory, that such a group of meteors of
the same velocity and mass should appear at the same height.
It is found that the beginning heights for meteors with normal

light curves can be well represented by the relationship ρv^3 = constant where ρ is the atmospheric density and v is the meteor velocity.

Among the meteors studies, a group of low-velocity meteors comprising 13 percent of the total are peculiar in the sense that they display an abrupt rise of light at the beginning of the trail. A typical meteor of this group will rise from below the plate limit to 1 magnitude above in less than $\frac{1}{60}$ sec. The shutter breaks often become invisible at the end of the trajectory (terminal blending). Both of these phenomena can be explained by a sudden increase of the effective surface area of the meteoroid by fragmentation into a number of smaller pieces. The differential deceleration of fragments of different sizes cause the meteoroid to spread along the trail and obscure the shutter breaks.

Meteors of this group do not obey the ρv^3 = constant law for beginning points. However, the point at which the burst takes place can be described in terms of a constant value of the dynamic pressure, $\rho v^2 = 2.5 \cdot 10^4$ dynes/sq cm (0.02 atmospheres). Quite likely we have here a measure of the weak crushing strength of meteoritic material.

The height corresponding to the observed value of ρv^3 is greater, at all meteor velocities, than the height corresponding to the observed ρv^2 value. Consequently,

if the above hypothesis is correct we should expect to
find occasionally a high-velocity meteor that first appears
normally at the proper value of ρv^3 and then shows a
fragmentation after its trajectory has carried it into the
range where crushing may take place. In 1949, Jacchia
reported 7 examples of high-velocity meteors that displayed
an abrupt increase in luminosity some time after their
appearance. The average value of ρv^2 at the point of
discontinuity of the light curve agrees with the value
obtained for those low-velocity meteors of this study
which obey the ρv^2 law.

The meteor wake has also been studied in some detail.
This phenomenon is characterized by a considerable amount of
luminosity in the shutter breaks of the meteor trail. A
study of those meteors reduced by the graphical method shows
that wake occurs predominately in low-velocity meteors. We
have also been able to show, conclusively, that the persistent
trains are produced almost entirely by meteors of high
velocity. Thus, it appears to be almost a certainty that
we must require some new process to form the wake. Jacchia's
concept of the continuous fragmentation of meteors offers
an obvious starting point.

We assume that small particles are detached from the
meteoroid and decelerate with respect to this parent body,
thus causing the luminosity of the meteor to extend over
a considerable distance at any given instant.

Such an assumption is sufficient to reproduce the observed wake but also necessitates that a large fraction of the light in the meteor be derived from the fragments and not the meteoroid directly. This is consistent with the observed values of the ablation constant, σ and with our observations showing the wake to be most noticeable in low-velocity meteors.